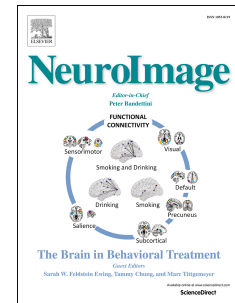


Journal Pre-proof



Can EEG and MEG detect signals from the human cerebellum?

Lau M. Andersen, Karim Jerbi, Sarang S. Dalal

PII: S1053-8119(20)30304-9

DOI: <https://doi.org/10.1016/j.neuroimage.2020.116817>

Reference: YNIMG 116817

To appear in: *NeuroImage*

Received Date: 10 September 2019

Revised Date: 17 March 2020

Accepted Date: 31 March 2020

Please cite this article as: Andersen, L.M., Jerbi, K., Dalal, S.S., Can EEG and MEG detect signals from the human cerebellum?, *NeuroImage*, <https://doi.org/10.1016/j.neuroimage.2020.116817>.

This is a PDF file of an article that has undergone enhancements after acceptance, such as the addition of a cover page and metadata, and formatting for readability, but it is not yet the definitive version of record. This version will undergo additional copyediting, typesetting and review before it is published in its final form, but we are providing this version to give early visibility of the article. Please note that, during the production process, errors may be discovered which could affect the content, and all legal disclaimers that apply to the journal pertain.

© 2020 The Author(s). Published by Elsevier Inc.

1 **Can EEG and MEG detect signals from the human cerebellum?**

2

3 Lau M. Andersen^{1,2*}, Karim Jerbi^{3,4}, Sarang S. Dalal¹

4

5 ¹ Center of Functionally Integrative Neuroscience, Aarhus University, Denmark

6 ² NatMEG, Karolinska Institutet, Stockholm, Sweden

7 ³ Computational and Cognitive Neuroscience Lab (CoCo Lab), Psychology Department, University
8 of Montreal, Montreal, QC, Canada

9 ⁴ MEG Unit, University of Montreal, Montreal, QC, Canada

10

11 * Corresponding author: lmandersen@cfin.au.dk

12 Abstract

13 The cerebellum plays a key role in the regulation of motor learning, coordination and timing, and
14 has been implicated in sensory and cognitive processes as well. However, our current knowledge of
15 its electrophysiological mechanisms comes primarily from direct recordings in animals, as
16 investigations into cerebellar function in humans have instead predominantly relied on lesion,
17 haemodynamic and metabolic imaging studies. While the latter provide fundamental insights into
18 the contribution of the cerebellum to various cerebellar-cortical pathways mediating behaviour, they
19 remain limited in terms of temporal and spectral resolution. In principle, this shortcoming could be
20 overcome by monitoring the cerebellum's electrophysiological signals. Non-invasive assessment of
21 cerebellar electrophysiology in humans, however, is hampered by the limited spatial resolution of
22 electroencephalography (EEG) and magnetoencephalography (MEG) in subcortical structures, i.e.,
23 deep sources. Furthermore, it has been argued that the anatomical configuration of the cerebellum
24 leads to signal cancellation in MEG and EEG. Yet, claims that MEG and EEG are unable to detect
25 cerebellar activity have been challenged by an increasing number of studies over the last decade.
26 Here we address this controversy and survey reports in which electrophysiological signals were
27 successfully recorded from the human cerebellum. We argue that the detection of cerebellum
28 activity non-invasively with MEG and EEG is indeed possible and can be enhanced with
29 appropriate methods, in particular using connectivity analysis in source space. We provide
30 illustrative examples of cerebellar activity detected with MEG and EEG. Furthermore, we propose
31 practical guidelines to optimize the detection of cerebellar activity with MEG and EEG. Finally, we
32 discuss MEG and EEG signal contamination that may lead to localizing spurious sources in the
33 cerebellum and suggest ways of handling such artefacts.

34 This review is to be read as a perspective review that highlights that it is indeed possible to measure
35 cerebellum with MEG and EEG and encourages MEG and EEG researchers to do so. Its added
36 value beyond highlighting and encouraging is that it offers useful advice for researchers aspiring to
37 investigate the cerebellum with MEG and EEG.

38 **1. Introduction**

39 In addition to its well-established role in the control and coordination of motor behaviour, the
40 cerebellum is involved in sensory processing (audition: Petacchi et al., 2005; retinotopy: van Es et
41 al., 2019) and cognitive tasks ranging from learning and memory to higher order cognitive control
42 processes (Ito, 1984; Thaut, 2003; Bellebaum and Daum, 2007; Strick et al., 2009; Casabona et al.,
43 2010; Stoodley et al., 2012; Buckner et al., 2013). King et al. (2019), using functional magnetic
44 resonance imaging (fMRI), recently showed that the cerebellum is involved in functions as diverse
45 as hand movements, saccades, divided attention, verbal fluency, autobiographical recall, word
46 comprehension, action observation, mental arithmetic, emotion processing and language processing,
47 among other functions. This is further evidence, if any were needed, that we simply cannot afford to
48 ignore the cerebellum in studies of human brain processes. However, the utility of noninvasive
49 electrophysiological techniques like electroencephalography (EEG) and magnetoencephalography
50 (MEG) for measuring cerebellar responses has not been clearly established, and sometimes even
51 explicitly discounted in textbooks (Tyner et al., 1989; Covey & Carter, 2015). Meanwhile, studies
52 employing EEG or MEG to delineate brain networks often do not consider the cerebellum as a
53 potential source of the measured responses. In this review, we argue for a more optimistic view on
54 EEG's and MEG's ability to detect cerebellar activity. We furthermore offer advice for how to
55 improve cerebellar recordings with MEG, hopefully providing a valuable tool that other researchers
56 aspiring to record the electrophysiological signals of the cerebellum can rely on.

57 Our current knowledge of the electrophysiological mechanisms that mediate cerebellar activity
58 comes mainly from direct recordings in animals. Investigations of the human cerebellum consist
59 predominantly of studies in patients with cerebellar lesions or studies tracking metabolic or
60 haemodynamic processes such as positron emission tomography (PET) and fMRI. In contrast to
61 electrophysiological recordings, these neuroimaging techniques only provide an indirect measure of
62 neural activity by monitoring local metabolic or haemodynamic responses. This notwithstanding,
63 neuroimaging studies using these modalities play a pivotal role in elucidating the functional role of
64 the cerebellum by unravelling its contribution to numerous tasks such as motor control, visually
65 guided behaviour and many cognitive tasks (Buckner, 2013). Because they monitor the activity of
66 the whole brain simultaneously, these imaging techniques are also used to examine the involvement
67 of the cerebellum in potential large-scale cerebral networks and to assess the functional-role of
68 cerebellar-thalamo-cortical pathways (Diedrichsen et al., 2019).

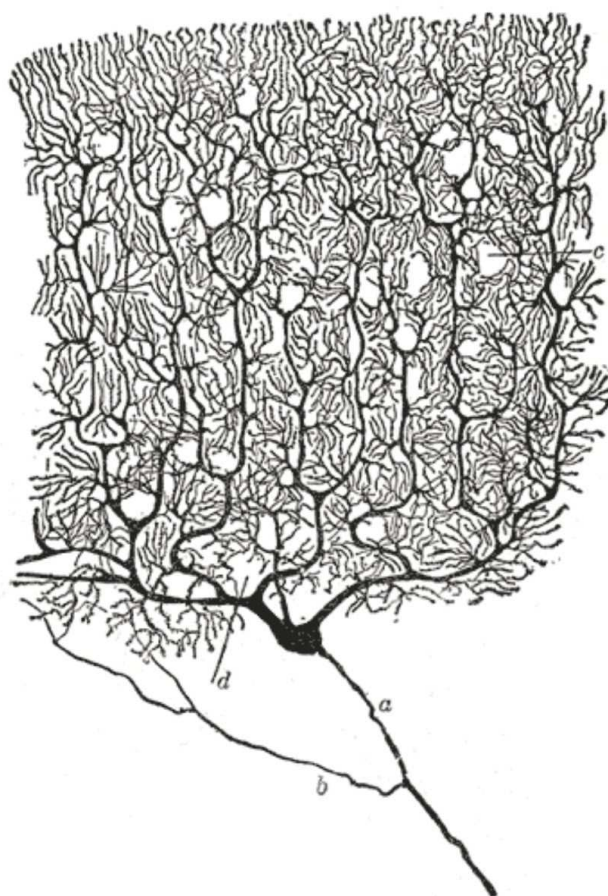
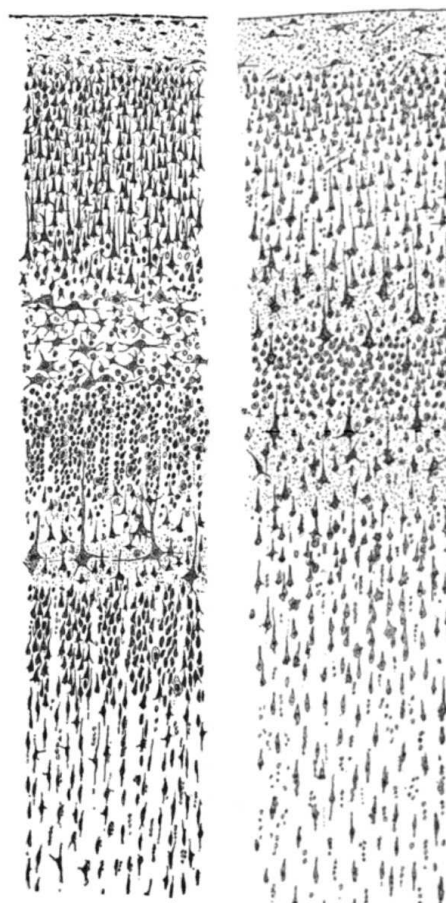
69 Nevertheless, the relatively sluggish nature of haemodynamic and metabolic responses remains a
70 severe limitation when it comes to investigating the precise temporal properties of cerebellar
71 activity. Recording signals from the cerebellum with temporal resolution comparable to that
72 obtained in electrophysiology (i.e., millisecond range) is crucial in order to correlate the measured

73 activity with behavioural parameters (such as reaction times or time-varying movement parameters)
 74 but also in order to compare activation latencies between cerebellum and other brain structures and
 75 finally to assess putative fine-grained synchronization properties between the cerebellum and
 76 various nodes of the involved cerebral network. To achieve the above, one would require a non-
 77 invasive technique that provides millisecond temporal resolution combined with whole-head
 78 coverage. EEG and MEG fulfil these requirements. While the former measures the electrical
 79 potentials on the scalp, the latter detects the minute magnetic signals generated on the surface by the
 80 same underlying cerebral generators (Hämäläinen et al., 1993). Both EEG and MEG record brain
 81 signals with millisecond resolution and currently available systems provide dense channel arrays
 82 with up to approximately 300 recording sites yielding full coverage of the head.

83 But do these methods provide the optimal spatiotemporal resolution at which to study the
 84 physiology of the human cerebellum? Unfortunately, the answer to this question is not
 85 straightforward. One problem lies with the poor spatial resolution of these techniques in deep
 86 structures, i.e., structures located far from the sensors. The distance from the sensor array and signal
 87 diffusion issues yield a low signal-to-noise ratio (SNR) and linear mixing at the individual
 88 recording sites. As a result, from a source estimation perspective, superficial sources (e.g., sources
 89 in primary auditory or somatosensory cortices) are easier to localize non-invasively with MEG or
 90 EEG than sources located in deeper brain structures (e.g., hippocampus or deeper substructures of
 91 the cerebellum). Furthermore, it has been speculated that the neuronal architecture of the cerebellar
 92 cortex may also be a specific limiting factor preventing detection of cerebellar sources with non-
 93 invasive methods due to signal cancellation. In general, MEG and EEG signals arise from (a) the
 94 spatial summation of underlying neural activity, i.e. many postsynaptic potentials in neighbouring
 95 dendrites with similar orientations, and (b) the temporal summation of these potentials, i.e. that
 96 these currents arise in the same short time interval. For the cerebellum, it has been thought that due
 97 to its more intricate folding relative to cerebral cortex, signals would cancel one another because
 98 neighbouring patches of cerebellum activation would result in currents of opposing orientation. This
 99 cancellation would preclude the spatial summation needed to generate a signal detectable with EEG
 100 or MEG. These potential difficulties, together with the attenuation of MEG and EEG signal strength
 101 with depth, has led to the prevailing view that MEG and EEG are not suitable for the detection of
 102 cerebellar activity. As a result, sources that appear to be localized in cerebellum are often suspected
 103 of being artefactual in origin or simply resulting from noisy data. Nonetheless, a small but
 104 increasing number of MEG and EEG studies report activations in the cerebellum in a range of tasks.
 105 So can MEG and EEG detect cerebellar activity after all? And if so, how can we optimize its
 106 detection and how can we rule out false positives? We believe that there is now sufficient evidence
 107 in the literature to address these questions.

109 2. Why is the detection of cerebellar activity with EEG and MEG a controversial issue?

110 It has been suggested that it has been difficult to record cerebellar activity with noninvasive EEG
111 (and by extension, MEG) since the neurons of the cerebellum are arranged in a “closed field”
112 configuration (Bantli, 1972). However, the arrangement of Purkinje cells in cerebellar cortex
113 (Ramón y Cajal, 1904) is very analogous to that of pyramidal cells in cerebral cortex (see Fig. 1)
114 and likely contribute to the scalp EEG/MEG signal. Studies on the turtle cerebellum have
115 demonstrated that an external magnetic field can be detected at a distance; a field of 1 pT was
116 detected at a distance of 17 mm when a cerebellar patch of 10 mm³ was activated (Okada et al.,
117 1987). The structure of the turtle cerebellar cortex is very similar to that of higher species, including
118 humans (Eccles, 2013). Buzsáki et al. (2012) furthermore highlight that the cerebellum has an
119 ordered structure, which would result in an open field configuration, but they note that cerebellar
120 activation is mainly local, meaning that corresponding external magnetic fields are weak. However,
121 in cases where synchronous activity is imposed on the cerebellum from outside itself, magnetic
122 fields strong enough to be detected by MEG can be generated, as for example is the case in epilepsy
123 (Kandel & Buzsáki, 1993). As synchronous activity may also be imposed on the cerebellum by
124 direct brain stimulation methods routinely used in neuroscience, it should, at least in principle, not
125 be impossible to detect cerebellum with MEG or EEG. MEG may be a more appropriate modality
126 than EEG, however, because MEG source localization suffers less from inaccuracies of the head
127 model than EEG source localization does. This makes source localization with MEG more precise
128 and accurate than with EEG given the same quality of head model (Hämäläinen et al., 1993,
129 Vorwerk et al., 2014, Wolters et al., 2006). Also, specifically for high-frequency oscillations, MEG
130 appears to capture them with higher fidelity than EEG does (Muthukumaraswamy & Singh, 2013).

A**B**

131

132 **Fig. 1: Similarities between Purkinje cells (cerebellum) and pyramidal cells (cerebral cortex)** **A**) a
 133 sketch of a Purkinje cell from the human cerebellum. **B**) a sketch of the pyramidal cells in sensory cortex and
 134 motor cortex of an adult, showcasing the different cortical layers. Both sketches are by Ramon y Cajal and
 135 are public domain: https://en.wikipedia.org/wiki/File:Purkinje_cell_by_Cajal.png and
 136 https://commons.wikimedia.org/wiki/File:Cajal_cortex_drawings.png

137 One reason that the cerebellum may not be visible to EEG or MEG may arise from some historical
 138 methodological limitations that have since been overcome. EEG and MEG studies employing
 139 event-related averaging, inherently optimized to distinguish phase-locked evoked activity, have
 140 rarely suggested cerebellum activation. Even experiments employing invasive recordings in animal
 141 cerebellum only occasionally report event-related potentials (ERPs) (e.g., Rowland & Jaeger, 2008);
 142 the vast majority of such studies instead report modulations of oscillatory activity (see de Zeeuw et
 143 al. (2008) for a review).

144 This suggests that the cerebellum may primarily exhibit oscillatory modulations that may not
 145 necessarily be phase-locked. Indeed, the classic experiments of Adrian (1935) [cat, 40-300 Hz],
 146 Dow (1938) [cat, 150-250 Hz], Ten Cate and Wiggers (1942) [cat, 50-230 Hz], and Pellet (1967)
 147 [guinea pig, 200-400 Hz] all demonstrated high-frequency oscillatory activity in the cerebellum.
 148 Niedermeyer & Uematsu (1974) observed low-frequency oscillations (1.5-6 Hz) in three human

149 Lennox-Gastaut syndrome patients implanted with cerebellar electrodes in an experimental attempt
 150 at stimulation treatment. de Solages et al. (2008) showed that the Purkinje cell layer produces 200
 151 Hz oscillations in Wistar rats, which seem to entrain unit firing; high-frequency LFPs in the
 152 molecular and granule cell layers were far less pronounced. More recently, Cheron & Cheron
 153 (2018) found that stimulation of the inferior olive in mice induced high-frequency oscillations (350
 154 Hz) in the cerebellum. Intracranial recordings from the human cerebellum are exceedingly rare, but
 155 Dalal et al. (2013) reviewed the sparse literature describing them, and re-analysed some key
 156 historical intracranial recordings of the human cerebellum, three published in Russian (Irger et al.
 157 1949a; 1949b; 1951) and one in French (Rétif 1964). In the studies by Irger et al., the human
 158 cerebellum exhibited spontaneous oscillations in the beta band range (15-30 Hz) and in both the
 159 low-gamma (35-50 Hz) and high-gamma (80-100 Hz) ranges. The recordings from Rétif (1964)
 160 furthermore revealed evidence of 250 Hz oscillations. The few intracranial recordings from the
 161 human cerebellum thus seem to correspond to the animal literature.

162 Perhaps the neuronal mechanisms or morphology of the cerebellum preclude robust production of
 163 phase-locked evoked responses, which would have given the impression that the cerebellum is
 164 silent to scalp EEG/MEG for several years until the revival of non-phase-locked analyses using
 165 time-frequency techniques. Indeed, more compelling MEG findings of cerebellar activity came
 166 about after techniques to perform time-frequency analysis in source space became more widely
 167 available (e.g., Gross et al., 2002; Dalal et al., 2008; Pollok et al., 2008; Schnitzler et al., 2009;
 168 Kennedy et al., 2011).

169 Sensor coverage may also be a factor. The traditional 10/20 EEG system and even state-of-the-art
 170 high-density electrode caps as well as most whole-head MEG systems may simply not provide
 171 sufficient spatial sampling over the regions where cerebellar signals may project, e.g., the top of the
 172 neck. This problem can be partially overcome using low-tech solutions, such as thoughtful
 173 placement of subjects in traditional MEG sensor arrays (perhaps with the head tilted more forward
 174 than usual for better cerebellar coverage at the expense of frontal coverage as in Hashimoto et al.
 175 (2003), or the use of additional free electrodes further down the neck to supplement an EEG cap.
 176 With the advent of on-scalp MEG techniques such as optically pumped magnetometers (OPMs)
 177 (Boto et al., 2017) and high critical temperature (high- T_c) SQUIDs (Pfeiffer et al., 2019), it is also
 178 becoming possible to place sensors freely, and thus place them as close as possible to the
 179 cerebellum, on the back of the head or possibly even into the mouth to approach it from the other
 180 side.

181 Source localization attempts have traditionally assumed a spherical head model fit to cerebral
 182 cortex, perhaps resulting in a poor fit with cerebellar cortex. Implementations of realistic head
 183 models usually neglect the cerebellum, either removing it completely or including it within the

184 same compartment as cerebral cortex. Additionally, techniques that assume sources to be oriented
 185 orthogonally to the cortical surface may need refinement for the cerebellum, as the cerebellum is
 186 less easily segmented. The cerebellum, due to its different morphology as well as its separation of
 187 cerebral cortex by thick dura mater (the cerebellar tentorium), may ultimately profit from realistic
 188 models that specifically take into account its electrical properties. Ramon et al. (2014) showed
 189 through simulation that head models that did not model the dura mater would overestimate the
 190 corresponding electric potential in EEG. Likewise, in MEG, given that secondary currents have been
 191 shown to contribute to the measured signal (Stenroos et al., 2014), this suggests that some
 192 improvement in MEG source localization may be achieved by modelling the cerebellar tentorium
 193 carefully.

194 Finally, it has long been speculated that the especially fine folding of the cerebellum may lead to
 195 substantial cancellation of signals recorded at the distance of MEG or EEG, due to the likelihood
 196 that sources on opposite sulci (with therefore opposing current flow) are simultaneously active.
 197 Recently, however, Samuelsson et al. (2020) quantified the degree of signal cancellation that can be
 198 expected, based on a boundary element model created of the cerebellum from a very high resolution
 199 ex vivo MRI (190 μ m voxel size at 9.4T). Their simulations estimate that the cerebellar signal
 200 should be attenuated only 30-60% on average relative to cerebral cortex, suggesting that the final
 201 signal strength of much of the cerebellum should still be well within the sensitivity limits of MEG
 202 and EEG.

203

204 **3. Previous reports and illustrative examples**

205 As mentioned earlier, the introduction of time-frequency analyses greatly increased the number of
 206 published findings on cerebellar activity stemming from mainly MEG recordings and some EEG
 207 recordings. We again emphasize that this spectral information would not be extractable using fMRI.
 208 Here, we will go through some of them in greater detail. We do not intend this to be a systematic
 209 review that includes all EEG and MEG papers that have been published on cerebellar activation, but
 210 rather a set of illustrative examples showcasing that MEG and EEG are not blind to the cerebellum.

211 *3.1 Motor tasks*

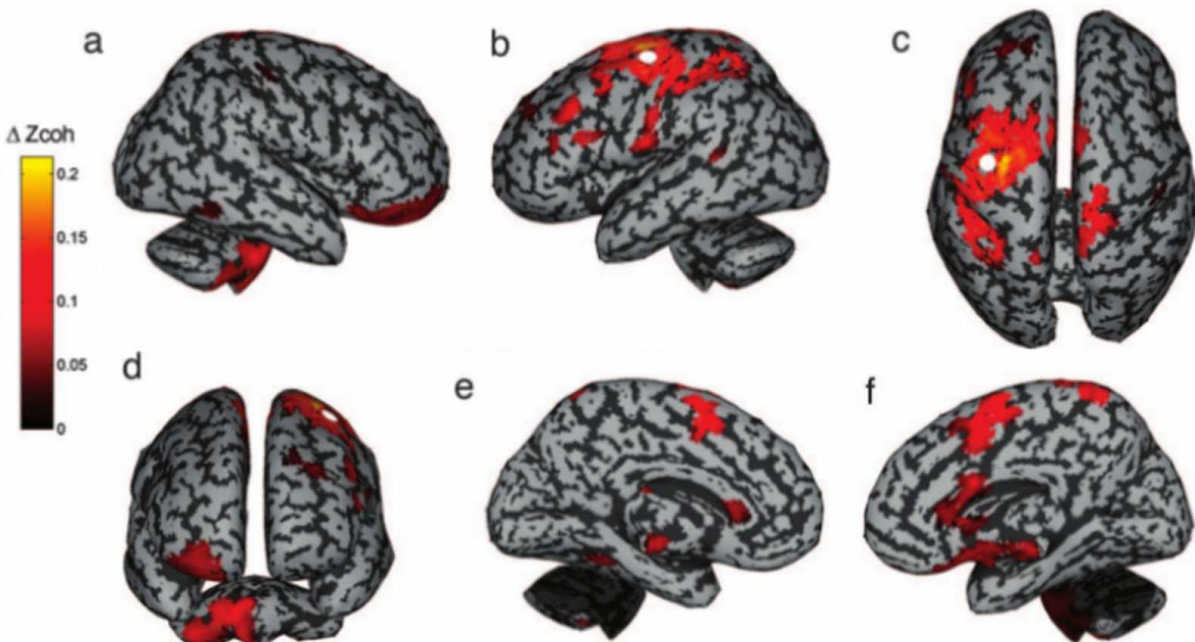
212 Gross et al. (2002), based on the application of Dynamic Imaging of Coherent Sources (DICS;
 213 Gross et al., 2001), found coherence between electromyography (EMG) resulting from a sinusoidal
 214 movement and MEG activity in the contralateral sensorimotor cortex, i.e., corticomuscular
 215 coherence. They then localized the brain areas coherently oscillating with sensorimotor cortex,
 216 among which they found ipsilateral cerebellum, thalamus and premotor cortex (PMC) engaged in a

217 feedback loop oscillating at a rhythm of 8-10 Hz, corresponding to natural discontinuities in
218 movement (Vallbo & Wessberg, 1993).

219 Pollok et al. (2005), also using DICS, extended the network to also include supplementary motor
220 area (SMA) and posterior parietal cortex (PPC), while Pollok et al. (2008) showed that anticipated
221 movements were related to an increase in coupling directed from cerebellar to thalamic to parietal
222 areas, i.e., cerebellum to cerebrum, whereas non-anticipated movements were related to an increase
223 in coupling direction from parietal areas to cerebellar areas, i.e., cerebrum to cerebellum. Pollok et
224 al. interpreted these two differentially directed couplings as anticipatory motor control and
225 mismatch detection, respectively. Jerbi et al. (2007) (Fig. 2) found that these cerebellar couplings to
226 motor cortex also encode the speed with which hand movements are made. All these studies take
227 advantage of using a peripheral EMG signal to reduce the space of potential coherence tests to be
228 made, by focusing the brain-to-brain coherence tests on only the brain region that included the
229 greatest corticomuscular brain-muscular coherence. Furthermore, they used simple motor tasks in
230 which the role of the cerebellum is undisputed and used individual MRs to create realistic head
231 models.

232 Wilson et al. (2010) (Fig. 3) found cerebellar activity in the beta band (15-30 Hz) before and after
233 movements. Finally, Dalal et al. (2008) furthermore found cerebellar activity in high gamma
234 frequencies (> 65 Hz) when subjects performed finger movements. Essentially, the same task was
235 used, but localization was based on the whole brain rather than on those coherent with the region
236 showing the greatest corticomuscular coherence.

237 Taken together, these studies provide consistent evidence that cerebellar activity can be detected in
238 MEG when simple motor movements are performed. Finally, a recent EEG study has used
239 distributed models to reconstruct phase-locked activity (Torres & Beardsley 2019) related to simple
240 flexions of the wrists. It remains to be seen whether the same could be done with MEG, which
241 would be very interesting, especially since these methods are very simple to apply.
242



243

244 **Fig. 2: Strength of task-based coherence with primary cortex as a reference:** subjects were to
 245 counteract the unpredictable movements of a cube rotating around its centre by moving a trackball. The
 246 kinematics of the trackball movement were registered and its coupling to the neural time series were
 247 estimated, using task-related Z-transformed coherence with M1 activity (white dot) as an outcome measure
 248 ($\Delta Zcoh$), showing coherence with the cerebellum. Figure from Jerbi et al. (2007).

249 In addition to detection of cerebellar activity in healthy participants, cerebellar activity has also
 250 been detected in patients with dysfunctional networks or motor pathologies.

251 Using DICS, and the same general methods that Gross et al. (2002) used, Timmermann et al. (2003)
 252 found oscillatory coherence between the EMG of the hand tremor of six Parkinson patients and
 253 their contralateral M1. Similar to Gross et al. (2002), they found evidence of coherence between
 254 contralateral M1 and ipsilateral cerebellum. Schnitzler et al. (2009) similarly found oscillatory
 255 coherence between the EMG of the hand and the contralateral M1 in eight patients with Essential
 256 Tremor. Again using DICS, they also found coherence between M1 and ipsilateral cerebellum.
 257 Similar results have been found for the tremor related to Wilson's disease (Südmeyer et al., 2006).

258 3.2 Somatosensation

259 MEG-based evidence for the cerebellum's involvement in pure somatosensation was reported
 260 earlier than the evidence for its involvement in motor control. Tesche and Karhu (1997) found that
 261 median nerve stimulation elicited cerebellar event-related responses, contrary to the motor studies
 262 above where only long-range EMG connectivity was reported. Furthermore, they found (2000) that
 263 omissions of otherwise expected somatosensory stimulations elicited oscillatory activity following
 264 the time point when the stimulation should have happened, and that cerebellar oscillatory activity

increased again before the following anticipated stimulation. Note that activity was not strictly speaking *localized* to the cerebellum in these studies, rather they estimated time courses for cerebellar sources given the assumption that there were sources there in the first place. As they also acknowledge, when time courses are estimated like this, it is possible that sources include activity generated at sources adjacent to the assumed source. Hashimoto et al. (2003), however, used a beamformer technique to localize median nerve stimulation evoked responses to the cerebellum. This study will be discussed more in-depth in a later section (Section 4) due to the importance of sensor coverage that it highlights.

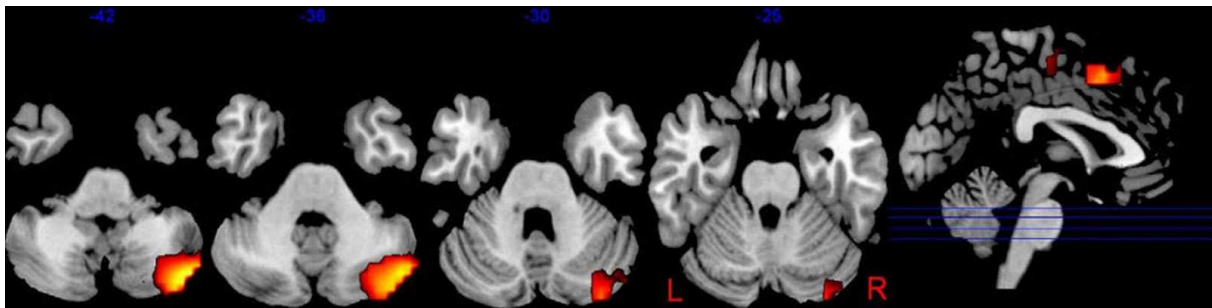
In addition to EMG, the kinematic signals of body movements have also been found to couple with the cerebellum in various contexts, a phenomenon referred to as *corticokinematic coherence* (CKC). For example, Marty et al. (2018) found that cerebellar activity entrains to the speed and kinematics of finger movements. A recent review of the relevant literature argues that CKC reflects proprioceptive spinocortical afferent signals, in contrast to CMC, which reflects corticospinal efferent signals (Bourguignon et al., 2019). The strategy here is very similar to using EMG as a peripheral signal to reduce the coherence source space (Gross et al., 2002)

Not relying on coupling, Andersen & Lundqvist (2019) (Fig. 4), using DICS, localized cerebellar oscillatory activity related to updating and maintaining expectations about somatosensation, ipsilateral to the stimulated hand in the theta and beta bands similar to the auditory study of Herrojo Ruiz (2017) discussed below. These two studies indicate that low-frequency cerebellar oscillations may be related to updating and maintaining expectations. An important difference between the study of Andersen & Lundqvist (2019) and the motor studies discussed above is that they are indirectly dependent on a peripheral reference signal usually EMG or kinematics of hand movement. In most of the motor studies cited, first coherence between an external reference, e.g. EMG, and M1 activity is established, and second the coherence between M1 and other areas are investigated. Andersen & Lundqvist (2019), although also using DICS, instead investigated the whole brain using the power maps output by DICS. This suggests that, using state-of-the-art MEG and source reconstruction methods, it is possible to retrieve cerebellar signals.

292 3.3 Audition

Using MEG, Ruiz et al. (2017), investigated auditory feedback related to motor movements (playing the piano). They provided feedback that was either expected (related to the movement) or unexpected (unrelated to the movement). When unexpected feedback was received, they found differences in the theta (3-7 Hz) and beta bands (15-30 Hz) to when expected feedback was received. Subsequently, they used common spatial pattern (CSP) analysis (Blankertz et al., 2008) to find the patterns of activity that were most strongly related to the differences between expected and

299 unexpected feedback and fitted dipoles to these patterns that revealed the cerebellum as a generator.
 300 Also using MEG, Cao et al. (2017), found that attenuation of self-generated tones, as indicated by
 301 the decrease of the auditory fields, was decreased when cerebellar activity was disrupted with TMS.
 302 They found that the cerebellar vermis was more active during actual attenuation, i.e. during the
 303 sham condition of the TMS. The source reconstruction was based on event-related fields (ERFs)
 304 using the eLORETA algorithm.



305 **Fig. 3: Pre-movement beta activation in cerebellar cortices.** Beta activation in ipsilateral cerebellar
 306 cortices following a flexion-extension movement. The maximum is in the inferior portions of ipsilateral
 307 cerebellum crus II. This figure is adapted from Wilson et al. 2010 with permission.

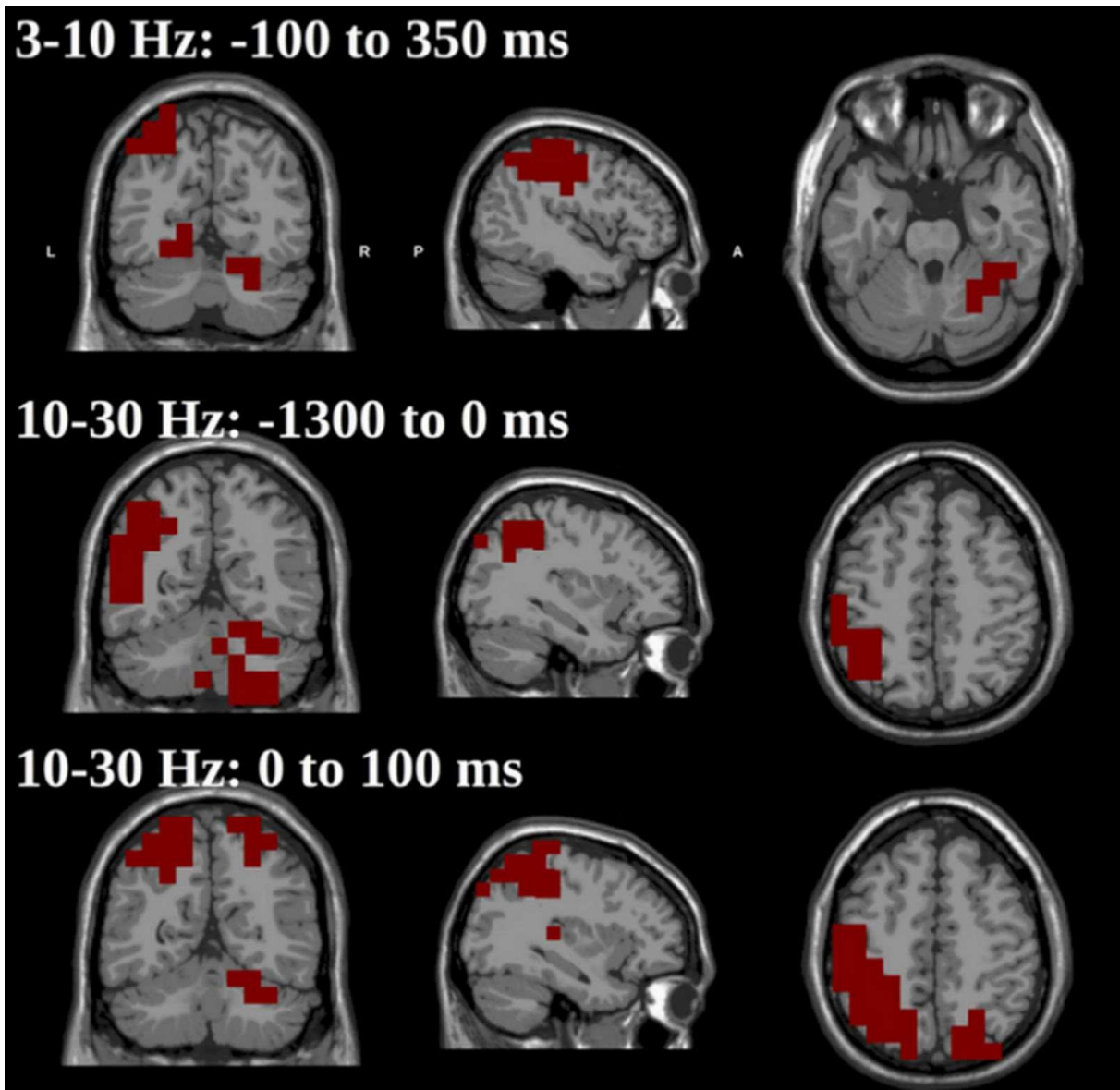
309 Using EEG, Reyes et al. (2005), found evidence of cerebellar involvement in the so-called 40 Hz
 310 auditory steady-state response (ASSR). The 40 Hz ASSR is an oscillation arising when tones are
 311 amplitude-modulated at a frequency of 40 Hz. Using the LORETA algorithm, they localized activity
 312 in the left cerebellum both when reconstructing the activity weighted and unweighted by an
 313 independent PET scan.

314 3.4 Visuomotor

315 Jousmäki et al. (1996) had subjects perform horizontal saccades every 3 s. Using a non-linear least
 316 squares fit, they fitted a two-dipole model in eight subjects, each resulting in one dipole localized to
 317 cerebellum and one localized to the posterior parietal cortex. These revealed evoked responses ~170
 318 ms after the onset of the saccade. In contrast to the studies of Tesche & Karhu (1997, 2000), these
 319 dipole fits represent a source localization and not estimates of time courses. Bourguignon et al.
 320 (2013) had subjects observe an experimenter moving his finger rhythmically (3 Hz). Using methods
 321 similar to Gross et al. (2001), DICS, reducing the coherence source space, they found that the motor
 322 cortices of subjects were coherently oscillating with the oscillating 3 Hz movement of the
 323 experimenter. Furthermore, they found that the primary motor cortex was coherently oscillating
 324 with cerebellum and V3 also at 3 Hz.

325 Using EEG in a visuomotor task, Cebolla et al. (2016) compared the alpha-mu (~8-12 Hz)
 326 oscillations in astronauts when they were either in a weightless state (in space) or on Earth. They
 327 found greater desynchronization of the mu rhythms when the astronauts were visually attending to

328 target stimuli when the astronauts were in space compared to when they were on Earth. Using a
 329 LORETA-style algorithm, cerebellum was revealed to contribute to this difference, possibly
 330 reflecting activation necessary for postural stabilization.
 331



332

333 **Fig. 4: Differences in cerebellar activation between expected and unexpected stimulations.** Subjects
 334 had their right index finger stimulated rhythmically (every 3 s). Every now and then a stimulation was omitted.
 335 The contrasts shown here indicate brain regions exhibiting significantly more power for *repeated stimulations*
 336 (a stimulation following another stimulation) than for *first stimulations* (a stimulation following an omission),
 337 where 0 ms refers to stimulation onset. This figure is adapted from Andersen & Lundqvist (2019) under the
 338 CC BY 4.0 licence.

339 *3.5 Cognition*

340 High-gamma oscillations (~60-180 Hz) in the cerebellum have also been implicated in decision
 341 making and introspection about decisions, perception and movement. Guggisberg et al. (2008)

342 found high-gamma oscillations in the cerebellum when participants make decisions related to
 343 numerical representation, explicit memory and self-representation. They specifically found that the
 344 left cerebellar hemisphere, together with the inferior parietal lobule, were the key structures
 345 involved with internally cued decisions. Guggisberg et al. (2011) found that the cerebellum was part
 346 of a network activated when participants were asked to introspect the timing of three kinds of
 347 events: phoneme perception, their own response decision, or the movement manifesting that
 348 decision. Both of these studies made use of the time-frequency beamformer technique introduced by
 349 Dalal et al. (2008), together with group statistics based on statistical non-parametric mapping
 350 (SnPM; Singh et al., 2003). Finally, Styliadis et al. (2015) using MEG found that oscillations (60-
 351 100 Hz) reflecting emotional arousal, emotional valence and their interaction were localized to
 352 distinct areas of the cerebellum using an LCMV (linearly constrained minimum-variance)
 353 beamformer. Moreover, they followed a temporal hierarchy with arousal being processed before
 354 valence.

355 3.6 Epilepsy

356 A few reports of cerebellar activity in epilepsy patients also exist. Niedermeyer & Uematsu (1975)
 357 presented three cases of epilepsy patients who were candidates for an experimental therapy of the
 358 time involving cerebellar stimulation. They exceptionally had recordings from a patient implanted
 359 with depth electrodes directly in the cerebellum simultaneously with scalp EEG, which showed that
 360 the cerebellum's activity, including apparently normal sleep spindles as well as seizure activity,
 361 could be shown in both the invasive and non-invasive recording leads. Mohamed et al. (2011)
 362 found, using an LCMV beamformer on MEG broadband activity (25-100 Hz), cerebellar activity 14
 363 s after ictal onset in the motor cortex in a four-year old boy. They discuss the possibility that the
 364 delayed cerebellar activity may play a modulatory role in seizure termination. Lascano et al. (2013),
 365 however, found evidence of a cerebellar lesion as the primary seizure generator in a 14-month old
 366 girl from high-density scalp EEG, which was subsequently confirmed by intracranial EEG
 367 performed immediately prior to surgical resection as well as freedom from seizures post-
 368 operatively. Finally, Elshoff et al. (2013) tested sources underlying the frequency spectrum in EEG
 369 epochs of 10 s recorded during seizures. Using DICS, they found cerebellar activity in 5 out of 11
 370 patients. The patients were between 1 and 19 years old (mean age: 9.6 years).

371 3.7 Resting state and network investigations

372 There is a great amount of resting state studies in the fMRI literature (van den Heuvel & Hulshoff
 373 Pol, 2010), and the cerebellum has also been found to be part of the so-called default mode network
 374 (Bernard et al., 2012; Sang et al., 2012). Brookes et al. (2011) used a combination of beamforming
 375 and independent component analysis (ICA) to retrieve the components making up the default mode

376 network. The components they found showed a great overlap with the components found in the
 377 fMRI literature. The cerebellar components specifically were found in the beta band range (13-30
 378 Hz). Wibral et al. (2011) investigated auditory short-term memory and found cerebro-cerebellar
 379 connections in the gamma band (60-120 Hz) using transfer entropy and DICS beamforming.
 380 Finally, Kujala et al. (2007) investigated phase coupling in a reading task and found cerebro-
 381 cerebellar couplings in the alpha band (8-13 Hz) during reading using a DICS beamformer.

382 3.8 Summary

383 Taken together, these studies show that cerebellar activity can, under certain circumstances, be
 384 detected with MEG and EEG. Many of the studies rely on an external reference, e.g., movement and
 385 observed movement, for establishing coherence between areas, and it is the coherence between
 386 oscillations that is detected rather than a standard task-related source activation. The studies of
 387 Jousmäki et al. (1996), Hashimoto et al. (2003), Cao et al. (2017) and Torres & Beardsley (2019)
 388 are also noteworthy for their detection of event-related fields in the cerebellum, where most other
 389 studies detect oscillatory responses.

390 **Table 1:** Studies reporting cerebellar findings using MEG or EEG sorted by domain, subject group, type of
 391 response and method for source localization. *Information obtained from personal communication

Authors and year	Modality	Domain	Subject group	Response	Source localization	Head model
Gross et al. (2002)	MEG	Motor	Neurotypical ($N=9$)	Long-range EMG connectivity	Beamformer (DICS)	Single shell head model (Nolte, 2003), based on individual MRs*
Timmermann et al. (2003)	MEG	Motor	Parkinson's Disease patients ($N=6$)	Long-range EMG connectivity	Beamformer (DICS)	Single shell head model (Nolte, 2003), based on individual MRs
Pollok et al. (2005)	MEG	Motor	Neurotypical ($N=10$)	Long-range EMG connectivity	Beamformer (DICS)	Single shell head model (Nolte, 2003), based on individual MRs
Jerbi et al. (2007)	MEG	Motor	Neurotypical ($N=15$)	Long-range connectivity	Minimum-norm estimate	Single sphere head models based on individual MRs*
Dalal et al. (2008)	MEG	Motor	Neurotypical ($N=12$)	Oscillations . ECoG used to validate results on	Beamformer	Multiple spheres model (Huang et al., 1999), based on individual MRs

				epilepsy patients (N=2)		
Pollok et al. (2008)	MEG	Motor	Neurotypical (N=11)	Long-range EMG connectivity	Beamformer (DICS)	Single shell head model (Nolte, 2003), based on individual MRs
Schnitzler et al. (2009)	MEG	Motor	Essential Tremor patients (N=8)	Long-range EMG connectivity	Beamformer (DICS)	Single shell head model (Nolte, 2003), based on individual MRs
Wilson et al. (2010)	MEG	Motor	Neurotypical children and adolescents (N=10)	Oscillations (beta band)	Beamformer (DICS)	Single shell head model, based on individual MRs*
Marty et al. (2018)	MEG	Motor	Neurotypical (N=11)	Long-range connectivity	Beamformer	Single shell head model (Gramfort et al., 2014), based on individual MRs
Torres & Beardsley (2019)	EEG	Motor	Neurotypical (N=15)	Event-related potentials	Minimum-norm estimate	Three-layered Boundary Element Method (OpenMEEG; Gramfort et al., 2010), based on template brain with individual electrode locations
Reyes et al. (2005)	EEG	Audition	Neurotypical (N=9)	Steady-state response	Minimum-norm estimate (LORETA)	Three-layered Boundary Element Method (Curry 4.5 Neuroscan Labs Inc., El Paso, TX), based on template brain with individual electrode locations
Ruiz et al. (2017)	MEG	Audition	Neurotypical (N=21)	Oscillations (theta and beta bands)	Dipole fitting	Single shell head model (Gramfort et al., 2014), based on individual MRs
Cao et al. (2017)	MEG	Audition	Neurotypical (N=10)	TMS and event-related fields	Minimum-norm estimate (eLORETA)	Single shell head model (Nolte, 2003), based on individual MRs
Tesche &	MEG	Somatosensatio	Neurotypic	Event-	Dipole time course	Single shell head

Karhu (1997)		n	al ($N=4$)	related fields.	estimation	model (Hämäläinen & Sarvas, 1989), based on individual MRs
Tesche & Karhu (2000)	MEG	Somatosensation	Neurotypical ($N=9$)	Event-related fields and oscillations.	Dipole time course estimation	Single shell head model (Hämäläinen & Sarvas, 1989), based on individual MRs
Hashimoto et al. (2003)	MEG	Somatosensation	Neurotypical ($N=12$)	Event-related fields	Beamformer	Single sphere head model, based on individual MRs
Andersen & Lundqvist (2019)	MEG	Somatosensation	Neurotypical ($N=20$)	Oscillations (theta and beta bands)	Beamformer (DICS)	Single shell head model (Nolte, 2003), based on individual MRs
Jousmäki et al. (1996)	MEG	Visuomotor	Neurotypical ($N=8$)	Event-related fields	Dipole fitting	Single sphere head model, based on individual MRs
Bourguignon et al. (2013)	MEG	Visuomotor	Neurotypical ($N=10$)	Long-range connectivity	Beamformer (DICS)	Not indicated
Cebolla et al. (2016)	EEG	Visuomotor	Astronauts in space and on Earth ($N=5$)	Oscillations (alpha band)	Minimum-norm estimate (swLORETA)	Boundary element method, layers not specified, based on template MR
Guggisberg et al. (2008)	MEG	Cognition	Neurotypical ($N=10$)	Oscillations (Gamma)	Beamformer	Multiple spheres head model, based on individual MRs
Guggisberg et al. (2011)	MEG	Cognition	Neurotypical ($N=11$)	Oscillations (Gamma)	Beamformer	Multiple spheres head model, based on individual MRs
Styliadis et al. (2015)	MEG	Emotion	Neurotypical ($N=12$)	Oscillations (Gamma)	Beamformer (SAM)	Multiple spheres head model, based on individual MRs
Niedermeyer & Uematsu (1975)	EEG	Epilepsy	Epileptic patients ($N=3$, ages 16, 18, 34)	Ictal and apparently normal sleep/drowsiness waveforms	Simultaneous intracranial EEG	None
Mohamed et al. (2011)	MEG	Epilepsy	Epileptic child ($N=1$)	Ictal and validated with iEEG	Beamformer	Not indicated

Lascano et al. (2013)	EEG	Epilepsy	Epileptic child ($N=1$)	Ictal and interictal.	Minimum-norm-estimate (LAURA)	Spherical Model with Anatomical Constraints (Spinelli et al., 2000) with individual MR
Elshoff et al. (2013)	EEG	Epilepsy	Epileptic children ($N=11$)	Ictal	Beamformer (DICS)	Five-concentric-spheres model with a single sphere for each layer corresponding to the white matter, grey matter, cerebral spinal fluid (CSF), skull and skin, based on individual MRs
Kujala et al. (2007)	MEG	Reading	Neurotypical ($N=9$)	Oscillations (alpha) and phase coupling	Beamformer (DICS)	Single-layer Boundary Element Method, based on individual MRs*
Brookes et al. (2011)	MEG	Resting state	Neurotypical ($N=10$)	Independent components	Beamformer	Not indicated
Wibral et al. (2011)	MEG	Auditory memory	Neurotypical ($N=22$)	Oscillations (Gamma) and transfer entropy	Beamformer	Single shell head model (Nolte, 2003), based on individual MRs
Lin et al. (2019)	Optically pumped magnetometers	Air-puffs to the eyes	Neurotypical ($N=3$)	Event-related fields and oscillations	Dipole fitting (event-related fields) and beamformer (oscillations)	Single shell head model (Nolte, 2003), based on individual MRs

392

393 **4. How can we enhance our ability to monitor cerebellum with MEG?**

394 In this section, we will cover methodological approaches that can enhance the chances of detecting
 395 cerebellar activity with MEG. We describe approaches that have successfully been used to detect
 396 cerebellar activity and discuss further promising strategies.

397 *4.1 Optimizing design (superficial targets and initial localization)*

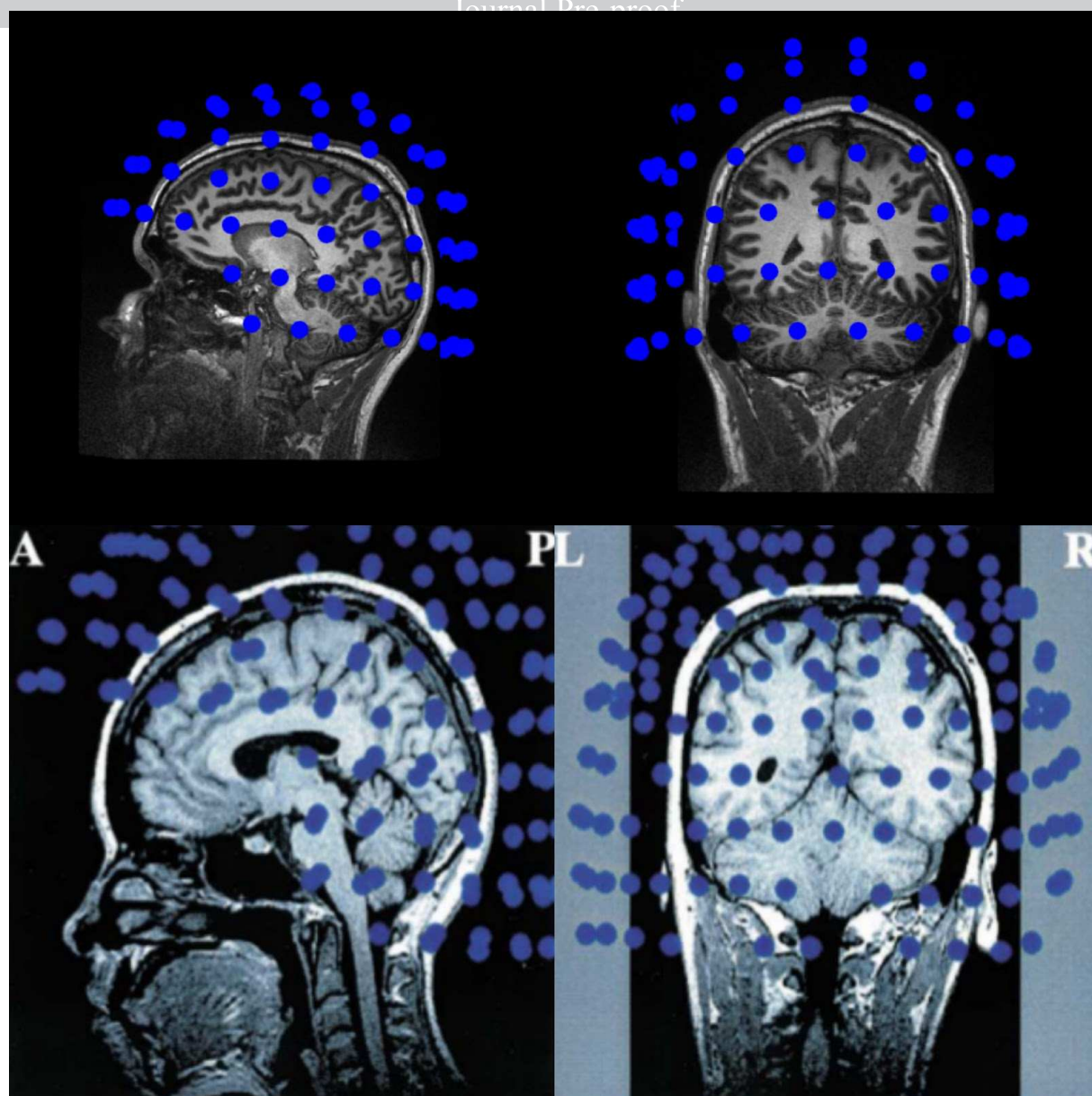
398 The signal of more anterior parts of the cerebellum is going to be comparatively small, purely due
 399 to the distance to the MEG sensors. If possible, one could aim to target cerebellar areas that are
 400 superficial, relatively speaking. This would of course require that studies based on other modalities
 401 had implicated the specific cerebellar region. For inspiration, one could look at the detailed
 402 functional mapping of King et al. (2019). A related strategy would be to use a paradigm that

robustly elicits a cerebellar response that can also be robustly localized. Using such a paradigm, a cerebellar source could be initially localized and thereafter its time course could be estimated for more subtle manipulations and variations of the localization paradigm. The question is though whether such a paradigm exists. A possible candidate might be the eye-blink conditioning paradigm. In eye-blink conditioning, performing an eye-blink is conditioned to the onset of tone (Conditioned Stimulus) which is followed by an air-puff to the eye (Unconditioned Stimulus). This conditioned response is dependent on an intact cerebellum (McCormick & Thompson 1984). Kirsch et al. (2003) found evidence of cerebellum's involvement in this response using MEG. Note however that their strategy is similar to that of Tesche and Karhu (1997, 2000) where they estimate the time course of assumed cerebellar sources. Recently, Lin et al. (2019) showed promising evidence of using the air-puff paradigm. This will be discussed further in section 4.7.

414 *4.2 Coverage of MEG sensor array or EEG coverage*

415 A recent study of Todd et al. (2018) extended the 10-20 layout with extra electrodes below electrode
 416 Oz . They very interestingly found that these “cerebellar” electrodes picked up high-frequency
 417 oscillations (> 100 Hz) that were unique to these electrodes and not found on the occipital
 418 electrodes above nor the splenius muscle electrodes below. This highlights the importance of
 419 actually covering the cerebellum such that signal can be picked up in the first place.

420 Hashimoto et al. (2003) investigated somatosensory fields evoked by median nerve stimulation
 421 using the Yokogawa MEGVISION with 160 axial gradiometers. Using a beamformer method
 422 (Sekihara et al. 2001), they were able to reconstruct fields as arising from the medial part of the
 423 cerebellum. As can be seen in Fig. 5, sensor coverage extended below the cerebellum, including the
 424 upper cervical spine. This seems to have been done by having subjects tilting their heads forwards
 425 relative to the helmet. This meant that some frontal coverage was sacrificed at the expense of being
 426 able to sample the cerebellum. This is a simple strategy that may be highly beneficial. As seen in the
 427 bottom row of Fig. 5, the cerebellum is not fully covered when the subject does not tilt their head.
 428



429

430 **Fig. 5: Tilting the head to obtain better sensor coverage of the cerebellum.** The upper panel shows a
 431 typical head placement in a modern MEG system, the Neuromag Triux, with its 102 sensor locations
 432 depicted in blue. While the cerebellum is partially covered with this positioning, tilting the head backwards
 433 relative to the sensor array may provide a more complete coverage of the cerebellum. Hashimoto et al.
 434 (2003) demonstrates such a positioning with a 160-channel Yokogawa MEG system, as seen in the lower
 435 panel, reproduced with permission (A=Anterior, P=Posterior, L=Left, R=Right).

436 *4.3 Careful artefact removal*

437 Cerebellar responses are susceptible to masking by or confounding with neck muscle EMG. It is
 438 therefore recommendable to record EMG from the major neck muscles. Especially, Minimum-
 439 Norm-Estimate-like and dipole fitting source reconstructions (Hämäläinen & Ilmoniemi, 1994)
 440 would benefit from this, since these will allocate all magnetic fields recorded by the sensors to the
 441 assumed source space. If the source space includes cerebellum, and neck muscle activity is not
 442 removed before source reconstruction, the neck muscle activity is likely to be source reconstructed

443 as spuriously arising from the cerebellum. Even in the presence of artefacts, beamformer methods
 444 will be useful since these reconstruct source activity independently at each assumed source location.
 445 This is done by creating a spatial filter that minimises contributions from other sources, brain and
 446 noise alike.

447 *4.4 Long-range coupling*

448 A successful strategy for localizing cerebellar activity has been to localize it based on its coherence
 449 with a “far-away” signal such as the EMG or kinematic signals of the foot or the hand
 450 (Bourguignon et al., 2019) as discussed in Section 3. Using long-range coupling adds a level of
 451 trustworthiness to the connectivity assessments, since short-range connectivity assessments have
 452 many interpretational pitfalls (Bastos and Schoffelen, 2016; Schoffelen and Gross, 2009). The
 453 paradigms of Gross’s and Jerbi’s groups have been very successful in applying this strategy (see
 454 Section 3). The kinds of paradigms that can be run with these kinds of strategies might be limited to
 455 sensory and motor paradigms, however.

456 *4.5 Reducing neocortical activity using Cortical Signal Suppression*

457 Samuelsson and Hämäläinen (2019) have developed the method of cortical signal suppression
 458 (CSS). The overall idea of this method is based on using unique features respectively of planar
 459 gradiometers and of magnetometers, as in the Neuromag system. Colloquially said, planar
 460 gradiometers are “near-sighted”, being maximally sensitive to signals arising from the cerebral
 461 cortex, whereas magnetometers are also sensitive to signals from beyond the cerebral cortex. By
 462 projecting out the signal shared between the magnetometers and planar gradiometers from the
 463 signal of the magnetometers alone, one can obtain a magnetometer signal that uniquely represents
 464 non-cerebral cortex. Applying this method to the auditory steady state response (ASSR), they were
 465 able to decrease the ASSR signal arising from cerebral cortex by 97%, while in turn increasing the
 466 ASSR signal arising subcortically by 10%. The method has not been applied to investigate
 467 cerebellar activity yet. Another interesting aspect about this method is that it does not require any
 468 special data acquisition procedures. Thus, already acquired data sets are likely to benefit from re-
 469 analysis using CSS if cerebellum or sub-cortical sources are expected.

470 *4.6 Improving anatomical models of cerebellum*

471 In beamformer applications, the orientations of the sources are normally not included in the source
 472 model. Instead, the direction that maximizes the beamformer’s output SNR is typically chosen as
 473 the source orientation, determined through an optimization based on singular value decomposition
 474 (Sekihara et al., 2004). However, Hillebrand and Barnes (2003) found that the signal of the
 475 beamformer could be improved if anatomical constraints were introduced, such that sources were

476 correctly oriented in the source model. The improvement in signal, however, is critically dependent
 477 on the co-registration error between MEG and MRI and the precision of the estimate of the
 478 orientation of the sources. Hillebrand and Barnes (2003) concluded that these errors need to be
 479 smaller than 2 mm and 10° respectively for these anatomical constraints. Regarding the co-
 480 registration error, several different strategies have been developed to reduce the error to less than 2
 481 mm, e.g., photogrammetry (Clausner et al. 2017), structured-light scanner (Zetter et al., 2019;
 482 Homölle & Oostenveld, 2019), and head casts (Meyer et al., 2017).

483 Regarding the estimation of source orientations, the typical anatomical constraint for MEG is to
 484 assume sources are orthogonal to the cortical surface extracted from anatomical T1 MRI scans.
 485 However, high-quality cortical surface extraction from 1.5T or 3T MRI is less tractable for the
 486 cerebellar cortex due to its thinness, leading to the unfortunate consequence that most available
 487 source analysis pipelines that depend on cortical surface information simply drop the cerebellum
 488 from the source space entirely. 7T MRI can yield sufficient resolution for reasonable extraction of
 489 the cerebellar cortical surface (Boillat et al., 2018). Samuelsson et al. (2020) emphasizes the
 490 importance of high-resolution cerebellar surface models, since they show that standard
 491 segmentations of the cerebellum give rise to an overestimation of the net cerebellar signal due to
 492 underestimation of signal cancellation, which can be avoided with high-resolution models. The
 493 high-resolution model also shows that more signal cancellation occurs in the cerebellum than in
 494 cerebral cortex, but that nonetheless cerebellar activity should be detectable using MEG and EEG.
 495 As an alternative to surface extraction from high-resolution scans, it has been suggested that neural
 496 fibre orientations may be derived from customized diffusion-weighted MRI (DWI) sequences at 3T;
 497 preliminary investigations suggest that this method can help distinguish activations of the visual
 498 cortex from the cerebellum (Dalal et al., 2018). It must be emphasized that invasive
 499 electrophysiological recordings of the cerebellum alongside MEG and/or EEG at a distance that
 500 provide actual information about the magnitude of signal cancellation in the cerebellum are still
 501 missing, but the modelling of Samuelsson et al. (2020) shows that signal cancellation in the
 502 cerebellum is not likely to make MEG and EEG recordings of cerebellum infeasible.

503 4.7 Speculation for the future - on scalp MEG

504 Several technologies are being developed where the ambition is to create whole-head arrays of on-
 505 scalp, or nearly on-scalp, MEG sensors. One alternative is to use high- T_c SQUIDs (Pfeiffer et al.,
 506 2019; Öisjöen et al., 2012). Successful recordings of somatosensory and auditory fields have been
 507 made using these (Andersen et al. 2017; Andersen et al. 2019; Pfeiffer et al. 2019). At present,
 508 arrays of up to 7 high- T_c SQUID magnetometers have been created. These can virtually be placed
 509 on the scalp (<1 mm). Another alternative, optically pumped magnetometers (OPMs), are already
 510 commercially available for assembly into small-scale systems suitable for MEG. Recordings with

511 20 OPMs have been conducted and can also be placed close to the scalp ~6.5 mm (Borna et al.
 512 2017; Boto et al. 2017). Since the pickup coil size of the magnetometers can be made smaller when
 513 moving towards the scalp, the spatial resolution will increase. This allows for sampling magnetic
 514 fields related to more focal brain activity than could be obtained with state-of-the-art MEG. As
 515 discussed earlier, one oft-mentioned reason that the cerebellum is purportedly not visible to MEG is
 516 that it is more finely folded than the cerebral cortex, resulting in signal cancellation. With finer
 517 spatial resolution, the problem of signal cancellation may be mitigated. Interestingly, the
 518 aforementioned Yokogawa system (Hashimoto et al. 2003) had a smaller pickup area 189 mm² than
 519 current CTF-systems (254 mm²) and Neuromag systems (441 mm²). In comparison, the size of the
 520 pickup coils in high-T_c SQUIDs is 81 mm² (Andersen et al. 2017; Andersen et al. 2019; Pfeiffer et
 521 al. 2019), and the equivalent pickup area modern OPMs is even smaller; for example, the surface
 522 area of the vapour cell of the QuSpin QZFM OPM is only 9 mm² (Osborne et al., 2018). These new
 523 technologies are likely to usher in a new exciting age for recordings of cerebellar MEG. In fact, a
 524 report already exists of OPMs being used to record evoked fields arising from the cerebellum (Lin
 525 et al., 2019). It furthermore seems likely that on-scalp technologies may be used to recover evoked
 526 responses from the cerebellum when doing classical median nerve stimulation as Hashimoto et al.
 527 (2003) did. On-scalp MEG may also improve SNR for high-frequency oscillations (Krishnaswamy
 528 et al. 2017) since it samples brain activity more sparsely than conventional MEG that samples the
 529 brain from a distance. It is important to note how bandwidth and sensitivity are inversely related in
 530 OPMs (Tierney et al., 2019). This has the implication that one cannot sample low- and high-
 531 frequency activity at the same time using the same sensor. On the other hand, some types of OPMs
 532 can be individually tuned such that their bandwidth is appropriate for picking up the relevant
 533 activity (Jiménez-Martínez et al., 2012). Bandwidth for high-T_c SQUIDs however is the same as for
 534 state-of-the MEG systems.

535 When designing the arrays, it is important that sensors are included in lower positions than the fixed
 536 low-T_c SQUID arrays currently include (Fig. 5). It is also feasible to build flexible arrays with both
 537 high-T_c SQUIDs (Riaz et al., 2017) and OPMs (Boto et al., 2019) meaning that one may be able to
 538 position the sensors according to what is optimal for one's present paradigm. Finally, using multiple
 539 layers of sensors may allow for better separation of cerebral cortex and deep sources akin to the use
 540 of reference sensors in the CTF (CTF MEG International Services LP. Coquitlam, BC, Canada)
 541 MEG systems. The reference sensors are used for noise cancellation (Boto et al., 2017), but could
 542 potentially be used to suppress cortical signals as well, related to the cortical signal suppression
 543 technique discussed above (Samuelsson et al., 2019).

544 4.8 Source localization of cerebellar MEG and cerebellar EEG respectively

545 There are well-known differences between MEG and EEG in terms of source localization and
 546 sensitivity. In the cerebral cortex, the sensitivity profiles of MEG and EEG differ in terms of MEG
 547 being insensitive to gyral activations - it may be thought that similar differences arise in the
 548 cerebellum, but due to the fine folding of the cerebellum, sulci and gyri are not well defined. As
 549 MEG source localization is less sensitive to inaccuracies in the head model than EEG source
 550 localization is, then, given identical head models, MEG source localization will thus likely be more
 551 precise and accurate than EEG source localization. Close approximations may work well for MEG,
 552 but less so for EEG.

553 Thus, careful attention especially needs to be given to EEG head models for them to be useful in
 554 corroborating cerebellar source localization. Careful attention to MEG head models will also be
 555 likely to improve cerebellar source localization, as discussed earlier, but will not be as crucial as in
 556 EEG. In terms of sensitivity, Samuelsson et al. (2020) also show that MEG is particularly sensitive
 557 to the posterior surface of the cerebellum. Paradigms that elicit activity close to the posterior surface
 558 of the cerebellum, such as the air-puff paradigm (e.g. Lin et al., 2019) and potentially
 559 touch/omission paradigms (e.g. Andersen & Lundqvist, 2019, may thus be especially worthwhile to
 560 investigate). Samuelsson et al. (2020) also show that EEG may be more sensitive to the anterior
 561 lobes of the cerebellum.

562 *4.9 Summary and general recommendations*

563 There are thus several strategies to employ to detect cerebellar activity. For any paradigm, however,
 564 one should increase the signal-to-noise ratio by acquiring as many trials as feasible. This
 565 necessitates a relatively simple paradigm without too many conditions. The results can be validated
 566 by ascertaining that any motor- or somatosensation-related responses arise from ipsilateral
 567 cerebellum. However, this requires both sides (e.g. left and right hands) to be tested – running
 568 counter to the idea of reducing the number of conditions. Experimental designs must therefore be
 569 optimized between these competing considerations.

570 *4.10 MEG's sensitivity to other structures outside neocortex*

571 In this section, we briefly consider evidence for the sensitivity of MEG and EEG to structures
 572 outside of neocortex. Our intention with this is to dispel the notion that MEG and EEG are
 573 exclusively generated by pyramidal cells near the surface of the cerebral cortex.

574 The auditory brainstem response is perhaps the most well-known evidence that sensors on the scalp
 575 are capable of measuring subcortical activity (Jewett et al., 1970). The auditory brainstem responses
 576 consists of responses to brief auditory stimuli, generated sequentially by the cochlea, auditory
 577 nerve, superior olivary complex, lateral lemniscus, and inferior colliculus. It is routinely measured

578 in the clinic with scalp electrodes, as a hearing test or measure of neural integrity. MEG sensors
 579 have also been able to capture the auditory brainstem response in experimental settings (Erné &
 580 Hoke, 1990; Parkkonen et al., 2009). It must be emphasized however that this requires many trials.
 581 Parkkonen et al. (2009) for instance used 16,000 trials, acquired over 30 minutes.

582 Ruzich et al. in their recent review (2019) found 37 MEG studies between the years 2005 to 2018
 583 that revealed robust hippocampal activity. Similarly, Pizzo et al. (2019) found evidence that using
 584 independent component analysis (ICA) hippocampal and amygdala activations could be found with
 585 MEG (6 out of 14 patients). Data from some patients (4 out of 14) even revealed evidence of a
 586 thalamic signal. These activations were independently verified using simultaneous intracranial EEG
 587 recordings. Even though less than half the patients had detectable signal, this demonstrates the
 588 possibility to record from otherwise deep regions. In another recent study (Müller et al., 2019),
 589 alpha band functional connectivity between thalamus and visual cortex was found in congenitally
 590 blind subjects. Especially the thalamic findings are interesting, since it is still controversial whether
 591 thalamus is detectable by MEG at all, due to its location close to the centre of the brain and its
 592 morphology. However, supporting the validity of Pizzo et al.'s (2019) and Müller et al.'s (2019)
 593 findings, Attal & Schwartz (2013), using a combination of simulations and real data, showed that
 594 MEG is sensitive to signal arising from hippocampus, amygdala and thalamus. They emphasize the
 595 need to have anatomically precise source spaces, orientation-constrained dipoles (if the area has a
 596 preferred direction) and a realistic estimate of dipole moment densities in different regions. We echo
 597 them in our advice to use anatomically precise models of the cerebellum. Thus, there is nothing
 598 about the depth *per se* that leaves cerebellum outside MEG's sensitivity range.

599

600 5. Conclusion

601 We conclude that it is indeed possible to detect EEG and MEG signals from the human cerebellum.
 602 Many studies using diverse methodologies have showcased EEG and MEG signals in different
 603 sensory domains such as audition, vision and somatosensation and during movements. There is also
 604 MEG-based evidence of the cerebellum being involved in more cognitive operations such as
 605 updating and maintaining sensory expectations, and in decision making.

606 Some limitations do exist at the moment however. The prime one is that the signal-to-noise ratio is
 607 low due to the larger distance between much of the cerebellum and the sensors (compared to the
 608 cerebrum). This means that we are likely to miss true activations of the cerebellum if the signal-to-
 609 noise ratio is low. Under favourable circumstances, e.g. high number of trials, optimized paradigms,
 610 facilitating coupling approaches, suppression of cortical activity, etc., this review indicates that
 611 cerebellar activation *can* be detected, just as many other deeper brain structures can, e.g.
 612 hippocampus, amygdala and thalamus. Even when we robustly detect cerebellar activation,

613 however, we still face the limitation of spatial resolution - with EEG and MEG it is hard to detect
 614 where exactly within the cerebellum we are. More precise anatomical models of the cerebellum
 615 may be useful for constraining the source reconstructions possible with EEG and MEG.

616 EEG and MEG studies of the cerebellum however have the immense utility of being able to resolve
 617 brain activity as it unfolds in real time compared to the sluggish responses of fMRI. This may be
 618 paramount in understanding the complexities and details of cerebellar function and dysfunction.
 619

620 **6. Acknowledgements**

621 LMA was supported by Carlsbergfondet (CF18-0843). KJ was supported by funding from the
 622 Canada Research Chairs program and a Discovery Grant (RGPIN-2015-04854) from the Natural
 623 Sciences and Engineering Research Council of Canada, a New Investigators Award from the Fonds
 624 de Recherche du Québec - Nature et Technologies (2018-NC-206005) and an IVADO-Apogée
 625 fundamental research project grant. SSD was supported by ERC Starting Grant 640448.
 626

627 **7. References**

628 Adrian, E.D. Discharge frequencies in the cerebral and cerebellar cortex. *J Physiol* (1934) vol. 83
 629 pp. 32P-33P

630 Andersen, L.M., Oostenveld, R., Pfeiffer, C., Ruffieux, S., Jousmäki, V., Hämäläinen, M.,
 631 Schneiderman, J.F., Lundqvist, D., 2017. Similarities and differences between on-scalp and
 632 conventional in-helmet magnetoencephalography recordings. *PLOS ONE* 12, e0178602.
 633 <https://doi.org/10.1371/journal.pone.0178602>

634 Andersen, L.M., Lundqvist, D., 2019. Somatosensory responses to nothing: An MEG study of
 635 expectations during omission of tactile stimulations. *NeuroImage* 184, 78–89.
 636 <https://doi.org/10.1016/j.neuroimage.2018.09.014>

637 Andersen, L.M., Pfeiffer, C., Ruffieux, S., Riaz, B., Winkler, D., Schneiderman, J.F., Lundqvist, D.,
 638 2019. On-scalp MEG SQUIDs are sensitive to early somatosensory activity unseen by conventional
 639 MEG. *bioRxiv* 686329. <https://doi.org/10.1101/686329>

640 Attal, Y., Schwartz, D., 2013. Assessment of subcortical source localization using deep brain
 641 activity imaging model with minimum norm operators: a MEG study. *PLoS ONE* 8, e59856.
 642 <https://doi.org/10.1371/journal.pone.0059856>

- 643 Bantli, H., 1972. Multi-electrode analysis of field potentials in the turtle cerebellum: an
 644 electrophysiological method for monitoring continuous spatial parameters. *Brain Research* 44, 676–
 645 679. [https://doi.org/10.1016/0006-8993\(72\)90334-4](https://doi.org/10.1016/0006-8993(72)90334-4)
- 646 Bastos, A.M., Schoffelen, J.-M., 2016. A Tutorial Review of Functional Connectivity Analysis
 647 Methods and Their Interpretational Pitfalls. *Front. Syst. Neurosci.* 9.
 648 <https://doi.org/10.3389/fnsys.2015.00175>
- 649 Bellebaum C, Daum I. Cerebellar involvement in executive control. *Cerebellum*. 2007;6(3):184–92.
- 650 Bernard, J.A., Seidler, R.D., Hassevoort, K.M., Benson, B.L., Welsh, R.C., Wiggins, J.L., Jaeggi,
 651 S.M., Buschkuhl, M., Monk, C.S., Jonides, J., Peltier, S.J., 2012. Resting state cortico-cerebellar
 652 functional connectivity networks: a comparison of anatomical and self-organizing map approaches.
 653 *Front. Neuroanat.* 6. <https://doi.org/10.3389/fnana.2012.00031>
- 654 Blankertz, B., Tomioka, R., Lemm, S., Kawanabe, M., Muller, K., 2008. Optimizing Spatial filters
 655 for Robust EEG Single-Trial Analysis. *IEEE Signal Processing Magazine* 25, 41–56.
 656 <https://doi.org/10.1109/MSP.2008.4408441>
- 657 Boillat, Y., Bazin, P.-L., O'Brien, K., Fartaria, M.J., Bonnier, G., Krueger, G., van der Zwaag, W.,
 658 Granziera, C., 2018. Surface-based characteristics of the cerebellar cortex visualized with ultra-high
 659 field MRI. *NeuroImage* 172, 1–8. <https://doi.org/10.1016/j.neuroimage.2018.01.016>
- 660 Borna, A., Carter, T.R., Goldberg, J.D., Colombo, A.P., Jau, Y.-Y., Berry, C., McKay, J., Stephen, J.,
 661 Weisend, M., Schwindt, P.D.D., 2017. A 20-channel magnetoencephalography system based on
 662 optically pumped magnetometers. *Phys. Med. Biol.* <https://doi.org/10.1088/1361-6560/aa93d1>
- 663 Boto, E., Meyer, S.S., Shah, V., Alem, O., Knappe, S., Kruger, P., Fromhold, T.M., Lim, M., Glover,
 664 P.M., Morris, P.G., Bowtell, R., Barnes, G.R., Brookes, M.J., 2017. A new generation of
 665 magnetoencephalography: Room temperature measurements using optically-pumped
 666 magnetometers. *NeuroImage* 149, 404–414. <https://doi.org/10.1016/j.neuroimage.2017.01.034>
- 667 Boto, E., Seedat, Z.A., Holmes, N., Leggett, J., Hill, R.M., Roberts, G., Shah, V., Fromhold, T.M.,
 668 Mullinger, K.J., Tierney, T.M., Barnes, G.R., Bowtell, R., Brookes, M.J., 2019. Wearable
 669 neuroimaging: Combining and contrasting magnetoencephalography and electroencephalography.
 670 *NeuroImage* 116099. <https://doi.org/10.1016/j.neuroimage.2019.116099>
- 671 Bourguignon, M., De Tiège, X., de Beeck, M.O., Van Bogaert, P., Goldman, S., Jousmäki, V., Hari,
 672 R., 2013. Primary motor cortex and cerebellum are coupled with the kinematics of observed hand
 673 movements. *NeuroImage* 66, 500–507. <https://doi.org/10.1016/j.neuroimage.2012.10.038>

- 674 Bourguignon, M., Jousmäki, V., Dalal, S.S., Jerbi, K., De Tiège, X., 2019. Coupling between human
 675 brain activity and body movements: Insights from non-invasive electromagnetic recordings.
 676 NeuroImage 203, 116177. <https://doi.org/10.1016/j.neuroimage.2019.116177>
- 677 Brookes, M.J., Woolrich, M., Luckhoo, H., Price, D., Hale, J.R., Stephenson, M.C., Barnes, G.R.,
 678 Smith, S.M., Morris, P.G., 2011. Investigating the electrophysiological basis of resting state
 679 networks using magnetoencephalography. PNAS 108, 16783–16788.
 680 <https://doi.org/10.1073/pnas.1112685108>
- 681 Buckner, R.L., 2013. The Cerebellum and Cognitive Function: 25 Years of Insight from Anatomy
 682 and Neuroimaging. Neuron 80, 807–815. <https://doi.org/10.1016/j.neuron.2013.10.044>
- 683 Buzsáki, G., Anastassiou, C.A., Koch, C., 2012. The origin of extracellular fields and currents —
 684 EEG, ECoG, LFP and spikes. Nature Reviews Neuroscience 13, 407–420.
 685 <https://doi.org/10.1038/nrn3241>
- 686 Cao L, Veniero D, Thut G, Gross J. Role of the Cerebellum in Adaptation to Delayed Action Effects.
 687 <https://doi.org/10.1016/j.cub.2017.06.074>
- 688 Casabona A, Bosco G, Perciavalle V, Valle MS. Processing of limb kinematics in the interpositus
 689 nucleus. Cerebellum. 2010 Mar;9(1):103-10.
- 690 Cebolla, A.M., Petieau, M., Dan, B., Balazs, L., McIntyre, J., Cheron, G., 2016. “Cerebellar
 691 contribution to visuo-attentional alpha rhythm: insights from weightlessness.” Scientific Reports 6,
 692 37824. <https://doi.org/10.1038/srep37824>
- 693 Cheron, J., Cheron, G., 2018. Beta-gamma burst stimulations of the inferior olive induce high-
 694 frequency oscillations in the deep cerebellar nuclei. European Journal of Neuroscience 48, 2879–
 695 2889. <https://doi.org/10.1111/ejn.13873>
- 696 Clausner, T., Dalal, S.S., Crespo-García, M., 2017. Photogrammetry-Based Head Digitization for
 697 Rapid and Accurate Localization of EEG Electrodes and MEG Fiducial Markers Using a Single
 698 Digital SLR Camera. Front. Neurosci. 11. <https://doi.org/10.3389/fnins.2017.00264>
- 699 Covey, E., Carter, M., 2015. Basic Electrophysiological Methods. Oxford University Press.
- 700 Dalal, S.S., Guggisberg, A.G., Edwards, E., Sekihara, K., Findlay, A.M., Canolty, R.T., Berger,
 701 M.S., Knight, R.T., Barbaro, N.M., Kirsch, H.E., Nagarajan, S.S., 2008. Five-dimensional
 702 neuroimaging: Localization of the time-frequency dynamics of cortical activity. Neuroimage 40,
 703 1686–1700. <https://doi.org/10.1016/j.neuroimage.2008.01.023>

- 704 Dalal, S.S., Osipova, D., Bertrand, O., Jerbi, K., 2013. Oscillatory activity of the human cerebellum:
 705 The intracranial electrocerebellogram revisited. *Neuroscience & Biobehavioral Reviews* 37, 585–
 706 593. <https://doi.org/10.1016/j.neubiorev.2013.02.006>
- 707 Dalal, S.S., Bailey, C.J., Westner, B.U., Lund, T.E., Petersen, M.V., 2018. Incorporating source
 708 orientations from DWI into MEG beamformer reconstructions of visual evoked responses
 709 [abstract]. Biomag 2018 meeting.
- 710 Diedrichsen, J., King, M., Hernandez-Castillo, C., Sereno, M., Ivry, R.B., 2019. Universal
 711 Transform or Multiple Functionality? Understanding the Contribution of the Human Cerebellum
 712 across Task Domains. *Neuron* 102, 918–928. <https://doi.org/10.1016/j.neuron.2019.04.021>
- 713 Dow, R.S., 1938. The electrical activity of the cerebellum and its functional significance. *J. Physiol.*
 714 (Lond.) 94, 67–86. <https://doi.org/10.1113/jphysiol.1938.sp003663>
- 715 Eccles, J.C., 2013. The Cerebellum as a Neuronal Machine. Springer Science & Business Media.
- 716 Elshoff, L., Muthuraman, M., Anwar, A.R., Deuschl, G., Stephani, U., Raethjen, J., Siniatchkin, M.,
 717 2013. Dynamic Imaging of Coherent Sources Reveals Different Network Connectivity Underlying
 718 the Generation and Perpetuation of Epileptic Seizures. *PLOS ONE* 8, e78422.
 719 <https://doi.org/10.1371/journal.pone.0078422>
- 720 Erné, S.N., Hoke, M., 1990. Short-latency evoked magnetic fields from the human auditory
 721 brainstem. *Adv Neurol* 54, 167–176.
- 722 van Es, D.M. van, Zwaag, W. van der, Knapen, T., 2019. Topographic Maps of Visual Space in the
 723 Human Cerebellum. *Current Biology* 29, 1689-1694.e3. <https://doi.org/10.1016/j.cub.2019.04.012>
- 724 Ferrari, C., Cattaneo, Z., Oldrati, V., Casiraghi, L., Castelli, F., D'Angelo, E., Vecchi, T., 2018. TMS
 725 Over the Cerebellum Interferes with Short-term Memory of Visual Sequences. *Scientific Reports* 8,
 726 6722. <https://doi.org/10.1038/s41598-018-25151-y>
- 727 Gramfort, A., Papadopoulo, T., Olivi, E., Clerc, M., 2010. OpenMEEG: opensource software for
 728 quasistatic bioelectromagnetics. *BioMedical Engineering OnLine* 9, 45.
 729 <https://doi.org/10.1186/1475-925X-9-45>
- 730 Gramfort, A., Luessi, M., Larson, E., Engemann, D., Strohmeier, D., Brodbeck, C., Parkkonen, L.,
 731 Hämäläinen, M., 2013. MNE software for processing MEG and EEG data. *NeuroImage*.
 732 <https://doi.org/10.1016/j.neuroimage.2013.10.027>

- 733 Gross, J., Kujala, J., Hämäläinen, M., Timmermann, L., Schnitzler, A., Salmelin, R., 2001. Dynamic
 734 imaging of coherent sources: Studying neural interactions in the human brain. PNAS 98, 694–699.
 735 <https://doi.org/10.1073/pnas.98.2.694>
- 736 Gross, J., Timmermann, L., Kujala, J., Dirks, M., Schmitz, F., Salmelin, R., Schnitzler, A., 2002.
 737 The neural basis of intermittent motor control in humans. PNAS 99, 2299–2302.
 738 <https://doi.org/10.1073/pnas.032682099>
- 739 Guggisberg, A.G., Dalal, S.S., Findlay, A.M., Nagarajan, S.S., 2008. High-frequency oscillations in
 740 distributed neural networks reveal the dynamics of human decision making. Front. Hum. Neurosci.
 741 2. <https://doi.org/10.3389/neuro.09.014.2007>
- 742 Guggisberg, A.G., Dalal, S.S., Schnider, A., Nagarajan, S.S., 2011. The neural basis of event-time
 743 introspection. Consciousness and Cognition, From Dreams to Psychosis: A European Science
 744 Foundation Exploratory Workshop 20, 1899–1915. <https://doi.org/10.1016/j.concog.2011.03.008>
- 745 Harrington, A., Hammond-Tooke, G.D., 2015. Theta Burst Stimulation of the Cerebellum Modifies
 746 the TMS-Evoked N100 Potential, a Marker of GABA Inhibition. PLOS ONE 10, e0141284.
 747 <https://doi.org/10.1371/journal.pone.0141284>
- 748 Hashimoto, I., Kimura, T., Tanosaki, M., Iguchi, Y., Sekihara, K., 2003. Muscle afferent inputs from
 749 the hand activate human cerebellum sequentially through parallel and climbing fiber systems.
 750 Clinical Neurophysiology 114, 2107–2117. [https://doi.org/10.1016/S1388-2457\(03\)00233-5](https://doi.org/10.1016/S1388-2457(03)00233-5)
- 751 Hämäläinen, M.S., Sarvas, J., 1989. Realistic conductivity geometry model of the human head for
 752 interpretation of neuromagnetic data. IEEE Transactions on Biomedical Engineering 36, 165–171.
 753 <https://doi.org/10.1109/10.16463>
- 754 Hämäläinen M, Hari R, Ilmoniemi RJ, Knuutila J, and Lounasmaa OV. 1993.
 755 Magnetoencephalography — theory, instrumentation, and applications to noninvasive studies of the
 756 working human brain, Rev. Mod. Phys. 65, 413–497
- 757 Hämäläinen, M.S., Ilmoniemi, R.J., 1994. Interpreting magnetic fields of the brain: minimum norm
 758 estimates. Medical & Biological Engineering & Computing 32, 35–42.
 759 <https://doi.org/10.1007/BF02512476>
- 760 Heller, L., van Hulsteyn, D.B., 1992. Brain stimulation using electromagnetic sources: theoretical
 761 aspects. Biophysical Journal 63, 129–138. [https://doi.org/10.1016/S0006-3495\(92\)81587-4](https://doi.org/10.1016/S0006-3495(92)81587-4)

- 762 Herrojo Ruiz M, Maess B, Altenmüller E, Curio G, Nukulin VV (2017). Cingulate and cerebellar
 763 beta oscillations are engaged in the acquisition of auditory-motor sequences. NeuroImage.
 764 <https://doi.org/10.1002/hbm.23722>
- 765 van den Heuvel, M.P., Hulshoff Pol, H.E., 2010. Exploring the brain network: A review on resting-
 766 state fMRI functional connectivity. European Neuropsychopharmacology 20, 519–534.
 767 <https://doi.org/10.1016/j.euroneuro.2010.03.008>
- 768 Hillebrand, A., Barnes, G.R., 2003. The use of anatomical constraints with MEG beamformers.
 769 NeuroImage 20, 2302–2313. <https://doi.org/10.1016/j.neuroimage.2003.07.031>
- 770 Homölle, S., Oostenveld, R., 2019. Using a structured-light 3D scanner to improve EEG source
 771 modeling with more accurate electrode positions. Journal of Neuroscience Methods 108378.
 772 <https://doi.org/10.1016/j.jneumeth.2019.108378>
- 773 Huang, M.X., Mosher, J.C., Leahy, R.M., 1999. A sensor-weighted overlapping-sphere head model
 774 and exhaustive head model comparison for MEG. Phys. Med. Biol. 44, 423–440.
 775 <https://doi.org/10.1088/0031-9155/44/2/010>
- 776 Irger, I.M., Koreisha, L.A., Tolmasskaia, E.S., 1949a. Electric potentials of the human cerebellum.
 777 Voprosy Nejrochirurgii 5, 34–38.
- 778 Irger, I.M., Koreisha, L.A., Tolmasskaia, E.S., 1949b. On spontaneous bioelectrical activity of the
 779 human cerebellum. Biulleten eksperimentalnoi biologii i meditsiny 27, 257–260.
- 780 Irger, I.M., Koreisha, L.A., Tolmasskaia, E.S., 1951. Investigation on the electric activity of
 781 phylogenetically different segments of the cerebellum in man and animal. Fiziologicheskiy zhurnal
 782 SSSR imeni I. M. Sechenova 37, 273–282.
- 783 Ito M. The cerebellum and neural control. New York: Raven; 1984.
- 784 Jewett, D.L., Romano, M.N., Williston, J.S., 1970. Human Auditory Evoked Potentials: Possible
 785 Brain Stem Components Detected on the Scalp. Science 167, 1517–1518.
 786 <https://doi.org/10.1126/science.167.3924.1517>
- 787 Jerbi, K., Lachaux, J.-P., N'Diaye, K., Pantazis, D., Leahy, R.M., Garnero, L., Baillet, S., 2007.
 788 Coherent neural representation of hand speed in humans revealed by MEG imaging. PNAS 104,
 789 7676–7681. <https://doi.org/10.1073/pnas.0609632104>

- 790 Jiménez-Martínez, R., Griffith, W.C., Knappe, S., Kitching, J., Prouty, M., 2012. High-bandwidth
 791 optical magnetometer. *J. Opt. Soc. Am. B, JOSAB* 29, 3398–3403.
- 792 <https://doi.org/10.1364/JOSAB.29.003398>
- 793 Jousmäki, V., Hämäläinen, M., Hari, R., 1996. Magnetic source imaging during a visually guided
 794 task. *Neuroreport* 7, 2961–2964.
- 795 Kandel, A., Buzsáki, G., 1993. Cerebellar neuronal activity correlates with spike and wave EEG
 796 patterns in the rat. *Epilepsy Research* 16, 1–9. [https://doi.org/10.1016/0920-1211\(93\)90033-4](https://doi.org/10.1016/0920-1211(93)90033-4)
- 797 Kennedy, J.S., Singh, K.D., Muthukumaraswamy, S.D., 2011. An MEG investigation of the neural
 798 mechanisms subserving complex visuomotor coordination. *International Journal of*

799 *Psychophysiology* 79, 296–304. <https://doi.org/10.1016/j.jpsycho.2010.11.003>

800 King, M., Hernandez-Castillo, C.R., Poldrack, R.A., Ivry, R.B., Diedrichsen, J., 2019. Functional
 801 boundaries in the human cerebellum revealed by a multi-domain task battery. *Nature Neuroscience*
 802 1. <https://doi.org/10.1038/s41593-019-0436-x>

803 Kirsch, P., Achenbach, C., Kirsch, M., Heinzmann, M., Schienle, A., Vaitl, D., 2003. Cerebellar and
 804 Hippocampal Activation During Eyeblink Conditioning Depends on the Experimental Paradigm: A
 805 MEG Study [WWW Document]. *Neural Plasticity*. <https://doi.org/10.1155/NP.2003.291>

806 Koch, G., Oliveri, M., Torriero, S., Salerno, S., Gerfo, E.L., Caltagirone, C., 2007. Repetitive TMS
 807 of cerebellum interferes with millisecond time processing. *Exp Brain Res* 179, 291–299.
 808 <https://doi.org/10.1007/s00221-006-0791-1>

809 Krishnaswamy, P., Obregon-Henao, G., Ahveninen, J., Khan, S., Babadi, B., Iglesias, J.E.,
 810 Hämäläinen, M.S., Purdon, P.L., 2017. Sparsity enables estimation of both subcortical and cortical
 811 activity from MEG and EEG. *PNAS* 114, E10465–E10474.
 812 <https://doi.org/10.1073/pnas.1705414114>

813 Kujala, J., Pammer, K., Cornelissen, P., Roebroek, A., Formisano, E., Salmelin, R., 2007. Phase
 814 Coupling in a Cerebro-Cerebellar Network at 8–13 Hz during Reading. *Cereb Cortex* 17, 1476–
 815 1485. <https://doi.org/10.1093/cercor/bhl059>

816 Lascano, A.M., Lemkadem, A., Granziera, C., Korff, C.M., Boex, C., Jenny, B., Schmitt-
 817 Mechelke, T., Thiran, J.-P., Garibotto, V., Vargas, M.I., Schaller, K., Seeck, M., Vulliemoz, S., 2013.
 818 Tracking the source of cerebellar epilepsy: Hemifacial seizures associated with cerebellar cortical
 819 dysplasia. *Epilepsy Research* 105, 245–249. <https://doi.org/10.1016/j.eplepsyres.2012.12.010>

- 820 Lin, C.-H., Tierney, T.M., Holmes, N., Boto, E., Leggett, J., Bestmann, S., Bowtell, R., Brookes,
 821 M.J., Barnes, G.R., Miall, R.C., 2019. Using optically-pumped magnetometers to measure
 822 magnetoencephalographic signals in the human cerebellum. *Journal of Physiology*.
 823 <https://doi.org/10.1113/JP277899>
- 824 McCormick, D.A., Thompson, R.F., 1984. Cerebellum: essential involvement in the classically
 825 conditioned eyelid response. *Science* 223, 296–299. <https://doi.org/10.1126/science.6701513>
- 826 Marty, B., Wens, V., Bourguignon, M., Naeije, G., Goldman, S., Jousmäki, V., De Tiège, X., 2018.
 827 Neuromagnetic Cerebellar Activity Entrain to the Kinematics of Executed Finger Movements.
 828 *Cerebellum* 17, 531–539. <https://doi.org/10.1007/s12311-018-0943-4>
- 829 Meyer, S.S., Bonaiuto, J., Lim, M., Rossiter, H., Waters, S., Bradbury, D., Bestmann, S., Brookes,
 830 M., Callaghan, M.F., Weiskopf, N., Barnes, G.R., 2017. Flexible head-casts for high spatial
 831 precision MEG. *Journal of Neuroscience Methods* 276, 38–45.
 832 <https://doi.org/10.1016/j.jneumeth.2016.11.009>
- 833 Mohamed, I.S., Otsubo, H., Ferrari, P., Ochi, A., Snead, O.C., Cheyne, D., 2011. Neuromagnetic
 834 cerebellar activation during seizures arising from the motor cortex. *Epilepsy Research* 96, 283–287.
 835 <https://doi.org/10.1016/j.epilepsyres.2011.06.003>
- 836 Muthukumaraswamy, S.D., Singh, K.D., 2013. Visual gamma oscillations: The effects of stimulus
 837 type, visual field coverage and stimulus motion on MEG and EEG recordings. *NeuroImage* 69,
 838 223–230. <https://doi.org/10.1016/j.neuroimage.2012.12.038>
- 839 Müller, F., Niso, G., Samiee, S., Ptito, M., Baillet, S., Kupers, R., 2019. A thalamocortical pathway
 840 for fast rerouting of tactile information to occipital cortex in congenital blindness. *Nat Commun* 10,
 841 1–9. <https://doi.org/10.1038/s41467-019-13173-7>
- 842 Niedermeyer, E., Uematsu, S., 1974. Electroencephalographic recordings from deep cerebellar
 843 structures in patients with uncontrolled epileptic seizures. *Electroencephalography and Clinical
 844 Neurophysiology* 37, 355–365. [https://doi.org/10.1016/0013-4694\(74\)90111-4](https://doi.org/10.1016/0013-4694(74)90111-4)
- 845 Nolte, G., 2003. The magnetic lead field theorem in the quasi-static approximation and its use for
 846 magnetoencephalography forward calculation in realistic volume conductors. *Phys. Med. Biol.* 48,
 847 3637. <https://doi.org/10.1088/0031-9155/48/22/002>
- 848 Okada, Y.C., Lauritzen, M., Nicholson, C., 1987. Magnetic field associated with neural activities in
 849 an isolated cerebellum. *Brain Research* 412, 151–155. [https://doi.org/10.1016/0006-8993\(87\)91451-X](https://doi.org/10.1016/0006-8993(87)91451-X)

- 851 Osborne, J., Orton, J., Alem, O., Shah, V., 2018. Fully integrated standalone zero field optically
 852 pumped magnetometer for biomagnetism, in: Steep Dispersion Engineering and Opto-Atomic
 853 Precision Metrology XI. Presented at the Steep Dispersion Engineering and Opto-Atomic Precision
 854 Metrology XI, International Society for Optics and Photonics, p. 105481G.
 855 <https://doi.org/10.1117/12.2299197>
- 856 Öisjöen, F., Schneiderman, J.F., Figueras, G.A., Chukharkin, M.L., Kalabukhov, A., Hedström, A.,
 857 Elam, M., Winkler, D., 2012. High-Tc superconducting quantum interference device recordings of
 858 spontaneous brain activity: Towards high-Tc magnetoencephalography. Applied Physics Letters
 859 100, 132601. <https://doi.org/10.1063/1.3698152>
- 860 Parkkonen, L., Fujiki, N., Mäkelä, J.P., 2009. Sources of auditory brainstem responses revisited:
 861 Contribution by magnetoencephalography. Human Brain Mapping 30, 1772–1782.
 862 <https://doi.org/10.1002/hbm.20788>
- 863 Pellet, J., 1967. L'électrocérébellogramme vermien au cours des états de veille et de sommeil. Brain
 864 Research 5, 266–270. [https://doi.org/10.1016/0006-8993\(67\)90092-3](https://doi.org/10.1016/0006-8993(67)90092-3)
- 865 Petacchi, A., Laird, A.R., Fox, P.T., Bower, J.M., 2005. Cerebellum and auditory function: an ALE
 866 meta-analysis of functional neuroimaging studies. Hum Brain Mapp 25, 118–128.
 867 <https://doi.org/10.1002/hbm.20137>
- 868 Pfeiffer, C., Ruffieux, S., Jönsson, L., Chukharkin, M.L., Kalaboukhov, A., Xie, M., Winkler, D.,
 869 Schneiderman, J.F., 2019. A 7-channel high-Tc SQUID-based on-scalp MEG system. bioRxiv
 870 534107. <https://doi.org/10.1101/534107>
- 871 Pizzo, F., Roehri, N., Villalon, S.M., Trébuchon, A., Chen, S., Lagarde, S., Carron, R., Gavaret, M.,
 872 Giusiano, B., McGonigal, A., Bartolomei, F., Badier, J.M., Bénar, C.G., 2019. Deep brain activities
 873 can be detected with magnetoencephalography. Nature Communications 10, 971.
 874 <https://doi.org/10.1038/s41467-019-08665-5>
- 875 Pollok, B., Gross, J., Kamp, D., Schnitzler, A., 2008. Evidence for Anticipatory Motor Control
 876 within a Cerebello-Diencephalic-Parietal Network. Journal of Cognitive Neuroscience 20, 828–840.
 877 <https://doi.org/10.1162/jocn.2008.20506>
- 878 Ramon, C., Gargiulo, P., Fridgeirsson, E.A., Haueisen, J., 2014. Changes in scalp potentials and
 879 spatial smoothing effects of inclusion of dura layer in human head models for EEG simulations.
 880 Front. Neuroeng. 7. <https://doi.org/10.3389/fneng.2014.00032>

- 881 Ramón y Cajal, S., 1904. La Textura del Sistema Nervioso del Hombre y los Vertebrados. Moya,
 882 Madrid.
- 883 Rétif, J., 1964. Étude de l'activité électrique spontanée du cervelet humain. Acta Neurologica et
 884 Psychiatrica Belgica 64, 825–831.
- 885 Reyes, S.A., Lockwood, A.H., Salvi, R.J., Coad, M.L., Wack, D.S., Burkard, R.F., 2005. Mapping
 886 the 40-Hz auditory steady-state response using current density reconstructions. Hearing Research
 887 204, 1–15. <https://doi.org/10.1016/j.heares.2004.11.016>
- 888 Riaz, B., Pfeiffer, C., Schneiderman, J.F., 2017. Evaluation of realistic layouts for next generation
 889 on-scalp MEG: spatial information density maps. Scientific Reports 7, 6974.
 890 <https://doi.org/10.1038/s41598-017-07046-6>
- 891 Rowland, N.C., Jaeger, D., 2008. Responses to Tactile Stimulation in Deep Cerebellar Nucleus
 892 Neurons Result From Recurrent Activation in Multiple Pathways. Journal of Neurophysiology 99,
 893 704–717. <https://doi.org/10.1152/jn.01100.2007>
- 894 Ruohonen, J., Ilmoniemi, R.J., 1998. Focusing and targeting of magnetic brain stimulation using
 895 multiple coils. Med. Biol. Eng. Comput. 36, 297–301. <https://doi.org/10.1007/BF02522474>
- 896 Ruzich, E., Crespo-García, M., Dalal, S.S., Schneiderman, J.F., 2019. Characterizing hippocampal
 897 dynamics with MEG: A systematic review and evidence-based guidelines. Hum Brain Mapp 40,
 898 1353–1375. <https://doi.org/10.1002/hbm.24445>
- 899 Samuelsson, J.G., Khan, S., Sundaram, P., Peled, N., Hämäläinen, M.S., 2019. Cortical Signal
 900 Suppression (CSS) for Detection of Subcortical Activity Using MEG and EEG. Brain Topogr.
 901 <https://doi.org/10.1007/s10548-018-00694-5>
- 902 Samuelsson, J.G., Sundaram, P., Khan, S., Sereno, M.I., Hämäläinen, M.S., 2020. Detectability of
 903 cerebellar activity with magnetoencephalography and electroencephalography. Human Brain
 904 Mapping. <https://doi.org/10.1002/hbm.24951>
- 905 Sang, L., Qin, W., Liu, Y., Han, W., Zhang, Y., Jiang, T., Yu, C., 2012. Resting-state functional
 906 connectivity of the vermal and hemispheric subregions of the cerebellum with both the cerebral
 907 cortical networks and subcortical structures. NeuroImage 61, 1213–1225.
 908 <https://doi.org/10.1016/j.neuroimage.2012.04.011>

- 909 Schnitzler, A., Müns, C., Butz, M., Timmermann, L., Gross, J., 2009. Synchronized brain network
 910 associated with essential tremor as revealed by magnetoencephalography. Movement Disorders 24,
 911 1629–1635. <https://doi.org/10.1002/mds.22633>
- 912 Schoffelen, J.-M., Gross, J., 2009. Source connectivity analysis with MEG and EEG. Hum. Brain
 913 Mapp. 30, 1857–1865. <https://doi.org/10.1002/hbm.20745>
- 914 Schutter, D.J.L.G., van Honk, J., 2006. An electrophysiological link between the cerebellum,
 915 cognition and emotion: Frontal theta EEG activity to single-pulse cerebellar TMS. NeuroImage 33,
 916 1227–1231. <https://doi.org/10.1016/j.neuroimage.2006.06.055>
- 917 Sekihara, K., Nagarajan, S.S., Poeppel, D., Marantz, A., Miyashita, Y., 2001. Reconstructing spatio-
 918 temporal activities of neural sources using an MEG vector beamformer technique. IEEE
 919 Transactions on Biomedical Engineering 48, 760–771. <https://doi.org/10.1109/10.930901>
- 920 Sekihara, K., Nagarajan, S.S., Poeppel, D., Marantz, A., 2004. Asymptotic SNR of scalar and vector
 921 minimum-variance beamformers for neuromagnetic source reconstruction. IEEE Trans Biomed Eng
 922 51, 1726–1734. <https://doi.org/10.1109/TBME.2004.827926>
- 923 Singh, K.D., Barnes, G.R., Hillebrand, A., 2003. Group imaging of task-related changes in cortical
 924 synchronisation using nonparametric permutation testing. NeuroImage 19, 1589–1601.
 925 [https://doi.org/10.1016/S1053-8119\(03\)00249-0](https://doi.org/10.1016/S1053-8119(03)00249-0)
- 926 de Solages, C., Szapiro, G., Brunel, N., Hakim, V., Isope, P., Buisseret, P., Rousseau, C., Barbour,
 927 B., Léna, C., 2008. High-Frequency Organization and Synchrony of Activity in the Purkinje Cell
 928 Layer of the Cerebellum. Neuron 58, 775–788. <https://doi.org/10.1016/j.neuron.2008.05.008>
- 929 Spinelli, L., Andino, S.G., Lantz, G., Seeck, M., Michel, C.M., 2000. Electromagnetic Inverse
 930 Solutions in Anatomically Constrained Spherical Head Models. Brain Topogr 13, 115–125.
 931 <https://doi.org/10.1023/A:1026607118642>
- 932 Stenroos, M., Hunold, A., Haueisen, J., 2014. Comparison of three-shell and simplified volume
 933 conductor models in magnetoencephalography. NeuroImage 94, 337–348.
 934 <https://doi.org/10.1016/j.neuroimage.2014.01.006>
- 935 Stoodley, C.J., Valera, E.M., Schmahmann, J.D., 2012. Functional topography of the cerebellum for
 936 motor and cognitive tasks: an fMRI study. NeuroImage 59, 1560–1570.
 937 <https://doi.org/10.1016/j.neuroimage.2011.08.065>

- 938 Strick PL, Dum RP, Fiez JA. Cerebellum and nonmotor function. *Annu Rev Neurosci.* 2009;32:413-
 939 34.
- 940 Styliadis, C., Ioannides, A.A., Bamidis, P.D., Papadelis, C., 2015. Distinct cerebellar lobules
 941 process arousal, valence and their interaction in parallel following a temporal hierarchy.
 942 *NeuroImage* 110, 149–161. <https://doi.org/10.1016/j.neuroimage.2015.02.006>
- 943 Südmeier, M., Pollok, B., Hefter, H., Gross, J., Butz, M., Wojtecki, L., Timmermann, L., Schnitzler,
 944 A., 2006. Synchronized brain network underlying postural tremor in Wilson's disease. *Movement*
 945 *Disorders* 21, 1935–1940. <https://doi.org/10.1002/mds.21104>
- 946 Ten Cate J., Wiggers N. (1942) On the occurrence of slow waves in the electrocerebellogram Arch.
 947 *Neerl. Physiol. l'Homme Anim.*, 26 (1942), pp. 433-435
- 948 Tesche, C.D., Karhu, J., 1997. Somatosensory evoked magnetic fields arising from sources in the
 949 human cerebellum. *Brain Research* 744, 23–31. [https://doi.org/10.1016/S0006-8993\(96\)01027-X](https://doi.org/10.1016/S0006-8993(96)01027-X)
- 950 Tesche, C.D., Karhu, J.J.T., 2000. Anticipatory cerebellar responses during somatosensory omission
 951 in man. *Hum. Brain Mapp.* 9, 119–142. [https://doi.org/10.1002/\(SICI\)1097-0193\(200003\)9:3<119::AID-HBM2>3.0.CO;2-R](https://doi.org/10.1002/(SICI)1097-0193(200003)9:3<119::AID-HBM2>3.0.CO;2-R)
- 953 Thaut MH. Neural basis of rhythmic timing networks in the human brain. *Ann N Y Acad Sci.* 2003
 954 Nov;999:364-73.
- 955 Tierney, T.M., Holmes, N., Mellor, S., López, J.D., Roberts, G., Hill, R.M., Boto, E., Leggett, J.,
 956 Shah, V., Brookes, M.J., Bowtell, R., Barnes, G.R., 2019. Optically pumped magnetometers: From
 957 quantum origins to multi-channel magnetoencephalography. *NeuroImage* 199, 598–608.
 958 <https://doi.org/10.1016/j.neuroimage.2019.05.063>
- 959 Timmermann, L., Gross, J., Dirks, M., Volkmann, J., Freund, H.-J., Schnitzler, A., 2003. The
 960 cerebral oscillatory network of parkinsonian resting tremor. *Brain* 126, 199–212.
 961 <https://doi.org/10.1093/brain/awg022>
- 962 Todd, N.P.M., Govender, S., Colebatch, J.G., 2018. The human electrocerebellogram (ECeG)
 963 recorded non-invasively using scalp electrodes. *Neuroscience Letters* 682, 124–131.
 964 <https://doi.org/10.1016/j.neulet.2018.06.012>
- 965 Torres, E., Beardsley, S., 2019. Cerebellar Source Localization using Event-Related Potentials in a
 966 Simple Motor Task, in: 2019 9th International IEEE/EMBS Conference on Neural Engineering

967 (NER). Presented at the 2019 9th International IEEE/EMBS Conference on Neural Engineering
 968 (NER), pp. 1076–1079. <https://doi.org/10.1109/NER.2019.8716916>

969 Tyner, F.S., Knott, J.R., Mayer, W.B., 1989. Fundamentals of EEG Technology: Clinical correlates.
 970 Lippincott Williams & Wilkins.

971 Vallbo, A.B., Wessberg, J., 1993. Organization of motor output in slow finger movements in man.
 972 The Journal of Physiology 469, 673–691. <https://doi.org/10.1113/jphysiol.1993.sp019837>

973 Vorwerk, J., Cho, J.-H., Rampp, S., Hamer, H., Knösche, T.R., Wolters, C.H., 2014. A guideline for
 974 head volume conductor modeling in EEG and MEG. NeuroImage 100, 590–607.
 975 <https://doi.org/10.1016/j.neuroimage.2014.06.040>

976 Wibral, M., Rahm, B., Rieder, M., Lindner, M., Vicente, R., Kaiser, J., 2011. Transfer entropy in
 977 magnetoencephalographic data: Quantifying information flow in cortical and cerebellar networks.
 978 Progress in Biophysics and Molecular Biology, BrainModes: The role of neuronal oscillations in
 979 health and disease 105, 80–97. <https://doi.org/10.1016/j.pbiomolbio.2010.11.006>

980 Wilson, T.W., Slason, E., Asherin, R., Kronberg, E., Reite, M.L., Teale, P.D., Rojas, D.C., 2010. An
 981 extended motor network generates beta and gamma oscillatory perturbations during development.
 982 Brain and Cognition 73, 75–84. <https://doi.org/10.1016/j.bandc.2010.03.001>

983 Wolters, C.H., Anwander, A., Tricoche, X., Weinstein, D., Koch, M.A., MacLeod, R.S., 2006.
 984 Influence of tissue conductivity anisotropy on EEG/MEG field and return current computation in a
 985 realistic head model: A simulation and visualization study using high-resolution finite element
 986 modeling. NeuroImage 30, 813–826. <https://doi.org/10.1016/j.neuroimage.2005.10.014>

987 Zetter, R., Ilvaininen, J., Parkkonen, L., 2019. Optical Co-registration of MRI and On-scalp MEG
 988 Scientific Reports 9, 5490. <https://doi.org/10.1038/s41598-019-41763-4>
 989 de Zeeuw, C.I., Hoebeek, F.E., Schonewille, M., 2008. Causes and Consequences of Oscillations in
 990 the Cerebellar Cortex. Neuron 58, 655–658. <https://doi.org/10.1016/j.neuron.2008.05.01>

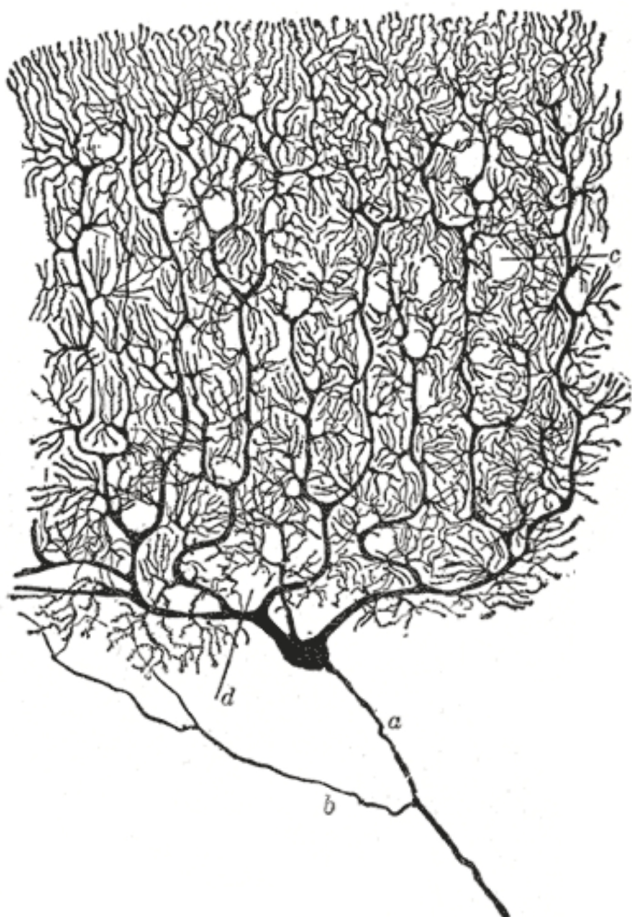
Authors and year	Modality	Domain	Subject group	Response	Source localization	Head model
Gross et al. (2002)	MEG	Motor	Neurotypical ($N=9$)	Long-range EMG connectivity	Beamformer (DICS)	Single shell head model (Nolte, 2003), based on individual MRs*
Timmermann et al. (2003)	MEG	Motor	Parkinson's Disease patients ($N=6$)	Long-range EMG connectivity	Beamformer (DICS)	Single shell head model (Nolte, 2003), based on individual MRs
Pollok et al. (2005)	MEG	Motor	Neurotypical ($N=10$)	Long-range EMG connectivity	Beamformer (DICS)	Single shell head model (Nolte, 2003), based on individual MRs
Jerbi et al. (2007)	MEG	Motor	Neurotypical ($N=15$)	Long-range connectivity	Minimum-norm estimate	Single sphere head models based on individual MRs*
Dalal et al. (2008)	MEG	Motor	Neurotypical ($N=12$)	Oscillations. ECoG used to validate results on epilepsy patients ($N=2$)	Beamformer	Multiple spheres model (Huang et al., 1999), based on individual MRs
Pollok et al. (2008)	MEG	Motor	Neurotypical ($N=11$)	Long-range EMG connectivity	Beamformer (DICS)	Single shell head model (Nolte, 2003), based on individual MRs
Schnitzler et al. (2009)	MEG	Motor	Essential Tremor patients ($N=8$)	Long-range EMG connectivity	Beamformer (DICS)	Single shell head model (Nolte, 2003), based on individual MRs
Wilson et al. (2010)	MEG	Motor	Neurotypical children and adolescents ($N=10$)	Oscillations (beta band)	Beamformer (DICS)	Single shell head model, based on individual MRs*
Marty et al. (2018)	MEG	Motor	Neurotypical ($N=11$)	Long-range connectivity	Beamformer	Single shell head model (Gramfort et al., 2014), based on individual MRs

Torres & Beardsley (2019)	EEG	Motor	Neurotypical (<i>N</i> =15)	Event-related potentials	Minimum-norm estimate	Three-layered Boundary Element Method (OpenMEG; Gramfort et al., 2010), based on template brain with individual electrode locations
Reyes et al. (2005)	EEG	Audition	Neurotypical (<i>N</i> =9)	Steady-state response	Minimum-norm estimate (LORETA)	Three-layered Boundary Element Method (Curry 4.5 Neuroscan Labs Inc., El Paso, TX), based on template brain with individual electrode locations
Ruiz et al. (2017)	MEG	Audition	Neurotypical (<i>N</i> =21)	Oscillations (theta and beta bands)	Dipole fitting	Single shell head model (Gramfort et al., 2014), based on individual MRs
Cao et al. (2017)	MEG	Audition	Neurotypical (<i>N</i> =10)	TMS and event-related fields	Minimum-norm estimate (eLORETA)	Single shell head model (Nolte, 2003), based on individual MRs
Tesche & Karhu (1997)	MEG	Somatosensation	Neurotypical (<i>N</i> =4)	Event-related fields.	Dipole time course estimation	Single shell head model (Hämäläinen & Sarvas, 1989), based on individual MRs
Tesche & Karhu (2000)	MEG	Somatosensation	Neurotypical (<i>N</i> =9)	Event-related fields and oscillations.	Dipole time course estimation	Single shell head model (Hämäläinen & Sarvas, 1989), based on individual MRs
Hashimoto et al. (2003)	MEG	Somatosensation	Neurotypical (<i>N</i> =12)	Event-related fields	Beamformer	Single sphere head model, based on individual MRs
Andersen & Lundqvist (2019)	MEG	Somatosensation	Neurotypical (<i>N</i> =20)	Oscillations (theta and beta bands)	Beamformer (DICS)	Single shell head model (Nolte, 2003), based on individual MRs
Jousmäki et al. (1996)	MEG	Visuomotor	Neurotypical (<i>N</i> =8)	Event-related fields	Dipole fitting	Single sphere head model, based on individual MRs
Bourguignon et al. (2013)	MEG	Visuomotor	Neurotypical (<i>N</i> =10)	Long-range connectivity	Beamformer (DICS)	Not indicated

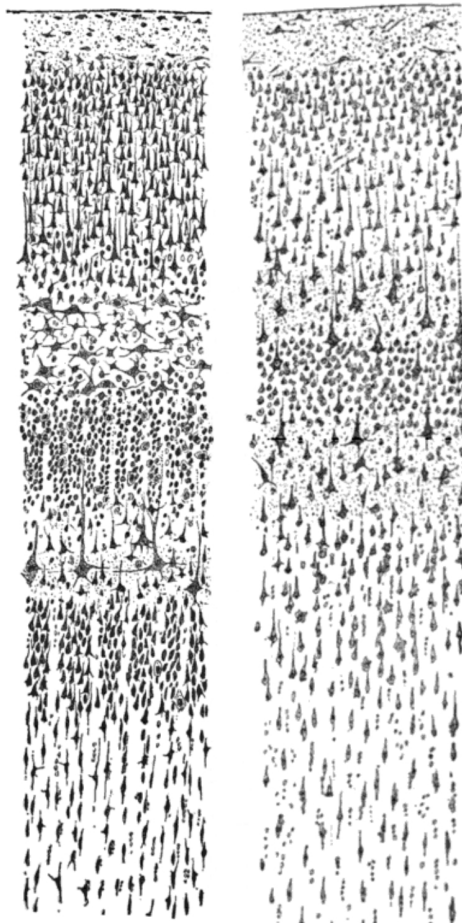
Cebolla et al. (2016)	EEG	Visuomotor	Astronauts in space and on Earth ($N=5$)	Oscillations (alpha band)	Minimum-norm estimate (swLORETA)	Boundary element method, layers not specified, based on template MR
Guggisberg et al. (2008)	MEG	Cognition	Neurotypical ($N=10$)	Oscillations (Gamma)	Beamformer	Multiple spheres head model, based on individual MRs
Guggisberg et al. (2011)	MEG	Cognition	Neurotypical ($N=11$)	Oscillations (Gamma)	Beamformer	Multiple spheres head model, based on individual MRs
Styliadis et al. (2015)	MEG	Emotion	Neurotypical ($N=12$)	Oscillations (Gamma)	Beamformer (SAM)	Multiple spheres head model, based on individual MRs
Niedermeyer & Uematsu (1975)	EEG	Epilepsy	Epileptic patients ($N=3$, ages 16, 18, 34)	Ictal and apparently normal sleep/drowsiness waveforms	Simultaneous intracranial EEG	None
Mohamed et al. (2011)	MEG	Epilepsy	Epileptic child ($N=1$)	Ictal and validated with iEEG	Beamformer	Not indicated
Lascano et al. (2013)	EEG	Epilepsy	Epileptic child ($N=1$)	Ictal and interictal.	Minimum-norm-estimate (LAURA)	Spherical Model with Anatomical Constraints (Spinelli et al., 2000) with individual MR
Elshoff et al. (2013)	EEG	Epilepsy	Epileptic children ($N=11$)	Ictal	Beamformer (DICS)	Five-concentric-spheres model with a single sphere for each layer corresponding to the white matter, grey matter, cerebral spinal fluid (CSF), skull and skin, based on individual MRs
Kujala et al. (2007)	MEG	Reading	Neurotypical ($N=9$)	Oscillations (alpha) and phase coupling	Beamformer (DICS)	Single-layer Boundary Element Method, based on individual MRs*
Brookes et al. (2011)	MEG	Resting state	Neurotypical ($N=10$)	Independent components	Beamformer	Not indicated

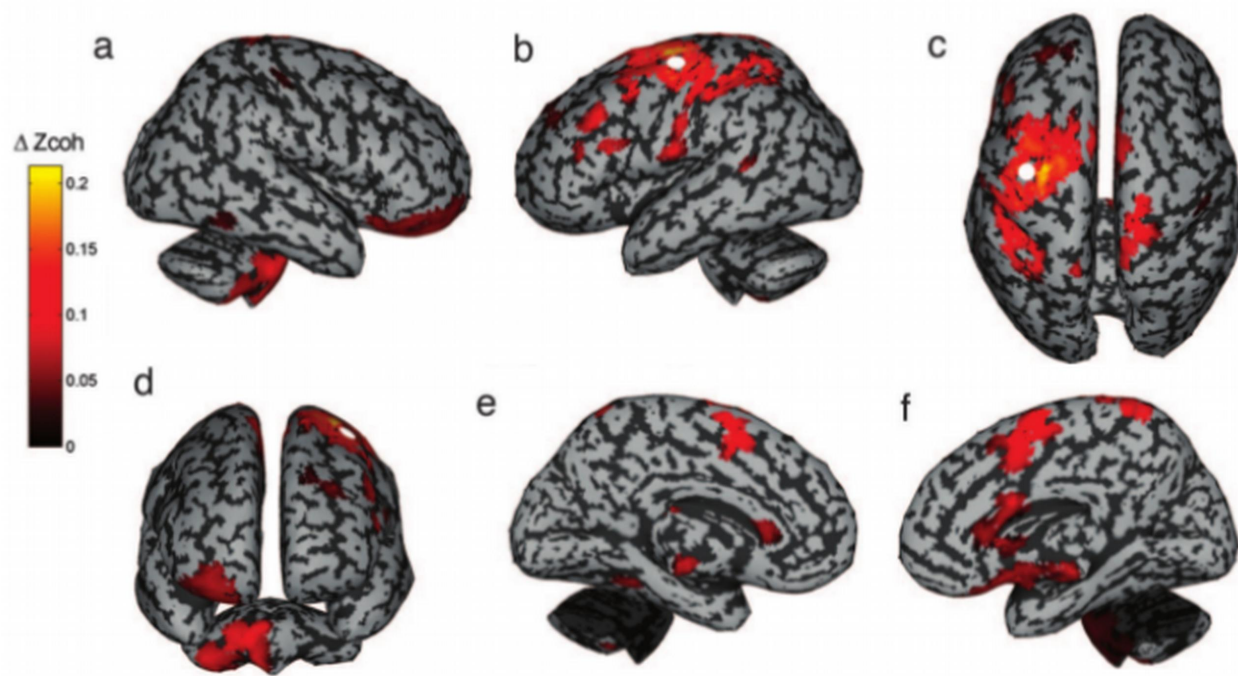
Wibral et al. (2011)	MEG	Auditory memory	Neurotypic al ($N=22$)	Oscillations (Gamma) and transfer entropy	Beamformer	Single shell head model (Nolte, 2003), based on individual MRs
Lin et al. (2019)	Optically pumped magnetomete rs	Air-puffs to the eyes	Neurotypic al ($N=3$)	Event- related fields and oscillations	Dipole fitting (event- related fields) and beamformer (oscillations)	Single shell head model (Nolte, 2003), based on individual MRs

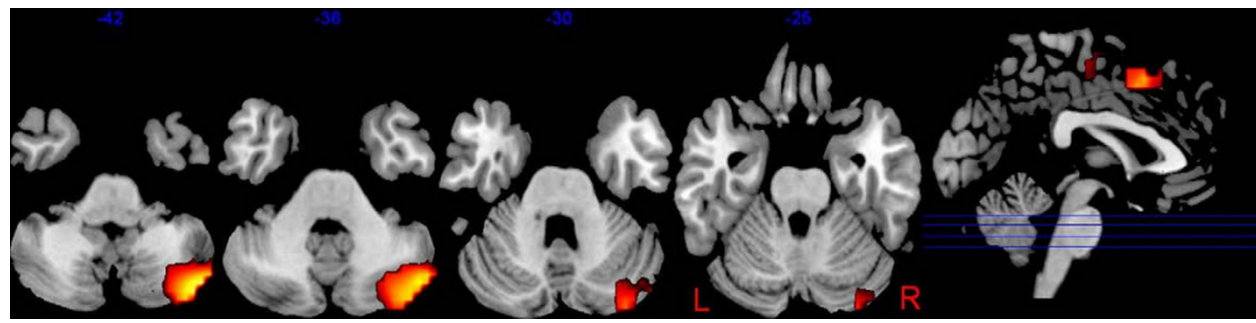
A



B



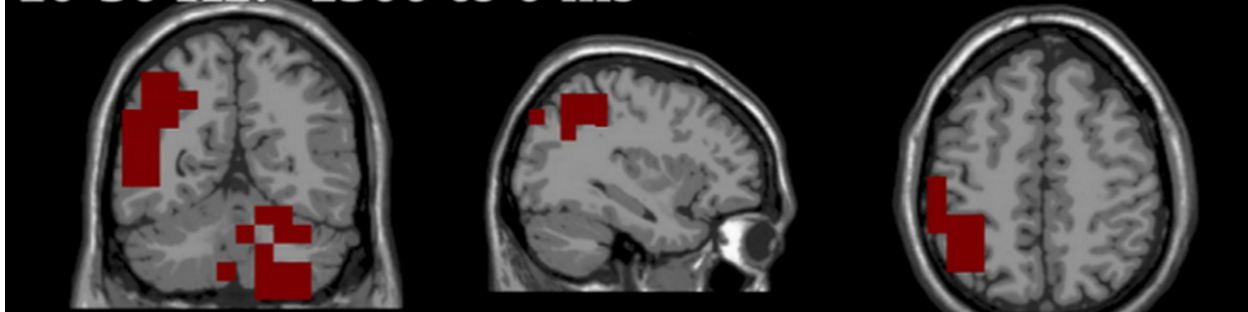




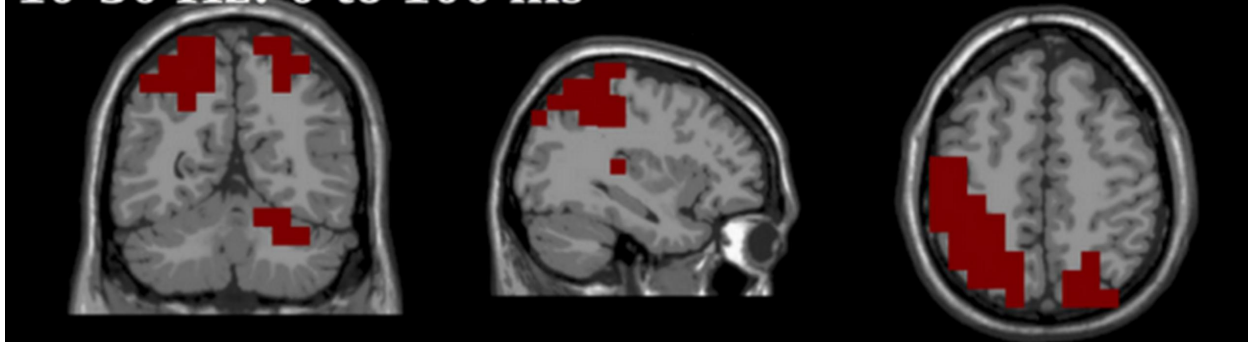
3-10 Hz: -100 to 350 ms

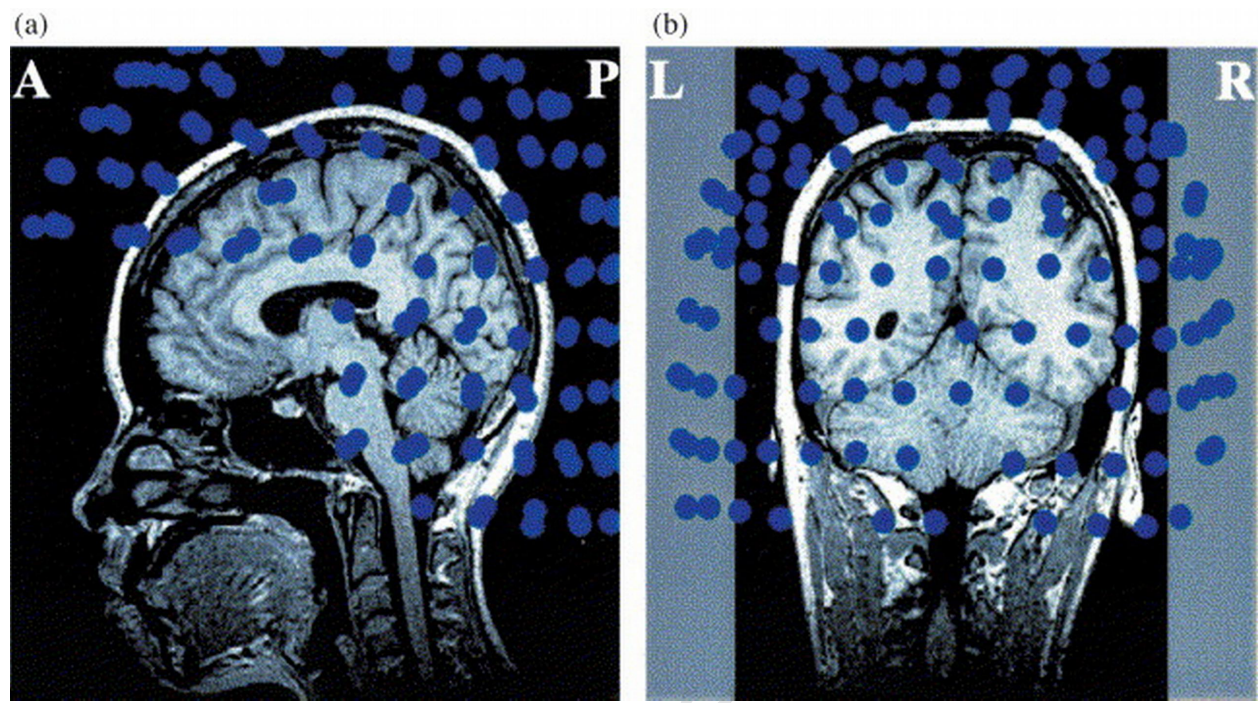


10-30 Hz: -1300 to 0 ms



10-30 Hz: 0 to 100 ms





Highlights:

- Electro- and magnetoencephalography can detect cerebellar signals
- We propose guidelines for detecting cerebellar signals non-invasively
- The cerebellum subserves several functions beyond mere motor processing